Quaternary International 714 (2024) 109587

Contents lists available at ScienceDirect

Quaternary International

journal homepage: www.elsevier.com/locate/quaint

The late Middle Pleistocene Zhongshan cave fauna from the Bubing Basin, southern China

Yaobin Fan [a], Yanyan Yao [a,b], Anne-Marie Bacon [c], Thijs van Kolfschoten [a,d], Jinyan Li [e], Christopher J. Bae [f], Wei Liao [a,**], Wei Wang [a,*]

[a] Institute of Cultural Heritage, Shandong University, 72 Jimo-Binhai Road, Qingdao, Shandong, 266237, China
[b] Center for Paleoanthropology Research, Anthropology Museum of Guangxi, Nanning, Guangxi, 530022, China
[c] Université Paris Cité, CNRS, UMR 8045 BABEL, 75012, Paris, France
[d] Faculty of Archaeology, Leiden University, the Netherlands
[e] Tiandong County Museum, Tiandong, Guangxi, 531500, China
[f] Department of Anthropology, University of Hawaii at Manoa, 2424 Maile Way 346 Saunders Hall, Honolulu, HI, 96822, USA

ARTICLE INFO

Keywords:
Middle-late pleistocene transition
Biochronological framework
Evolutionary history
Faunal diversity
Late Pleistocene

ABSTRACT

The karstic caves in the Bubing Basin, Guangxi, southern China, contain abundant Quaternary mammalian fossils. These cave sites are located at varying altitudes that have been roughly correlated with chronological age (higher caves are older, lower caves are younger). A growing number of recent studies have established a regional biochronological sequence for these Bubing caves from the Early to the Late Pleistocene. Here, we describe a new mammalian assemblage from the Zhongshan Cave, that dates to the late Middle Pleistocene - Marine Isotope Stage 6 (191–130 ka). The age is supported by minimum ages derived from U-series dating of the deposits, and the ESR/U-series dating of one *Rhinoceros* tooth (~184 ka). The Zhongshan mammalian assemblage, comprising 33 taxa of large-sized mammals, belongs to the Middle Pleistocene "*Ailuropoda-Stegodon*" faunal unit and, in this respect, most closely resembles the Ganxian fauna (362–168.9 ka). The high diversity and abundance of ruminant Artiodactyla (versus Perissodactyla) in the Zhongshan fauna suggest a diversity of forest to more open habitats in the Bubing Basin during this period.

The Zhongshan fauna fills a gap in the biochronological framework of southern China, offering new insights into the evolutionary history of some mammalian lineages in the Bubing Basin. Overall, data indicate major changes in the Early to Late Pleistocene faunal sequence, particularly with more turnover during the Early-Middle Pleistocene transition compared to the Middle-Late Pleistocene transition.

Comparison between faunas from the Bubing Basin with those from sites in the Chongzuo area, also in Guangxi, southern China, highlights two major phases in the general decline of large-sized mammals during the Middle to Late Pleistocene transitional period. In that respect, our results provide an updated biochronological background for further analyses of the region.

1. Introduction

The karstic cave sites of the Bubing Basin, Guangxi, southern China, yield plentiful mammalian assemblages associated in some caves (e.g. Luna Cave) with modern human teeth (e.g. Li et al., 1985; Chen et al., 2002; Wang et al., 2007, 2009, 2014a; Bae et al., 2014; Liang et al., 2022; Fan et al., 2022a; Liao et al., 2022). These assemblages of large mammal fossils have been assigned to the "*Ailuropoda-Stegodon*" faunal unit (*sensu lato*) (Matthew and Granger, 1923; Colbert, 1943; Colbert and Hooijer, 1953) that was widespread across the Southeast Asian mainland, including southern China during the Pleistocene (e.g. Pope et al., 1981; Patte, 1928; de Terra, 1938; Norton et al., 2010; Bocherens et al., 2017). In southern China, the Quaternary fossiliferous records are particularly abundant in the Bubing Basin and the Chongzuo area.

Palaeontological studies have revealed that these cave faunas represent different biochronological phases (e.g. Bien and Chia, 1938; Zhou, 1957; Ji, 1977; Bacon et al., 2011) based on different proportions of extinct and extant taxa. Using palaeomagnetic, isotopic and

* Corresponding author.
** Corresponding author.
E-mail addresses: liaowei@sdu.edu.cn (W. Liao), wangw@sdu.edu.cn (W. Wang).

https://doi.org/10.1016/j.quaint.2024.11.005
Received 13 March 2024; Received in revised form 11 July 2024; Accepted 9 November 2024
Available online 22 November 2024

luminescence dating methods, a chronological framework of mammalian faunas has been progressively refined in the Bubing Basin from the Early Pleistocene to the Late Pleistocene: Chuifeng cave (1.92 ± 0.14 Ma; Shao et al., 2014) and Mohui cave (1.95–1.78 Ma; Ma et al., 2017) dated to the Early Pleistocene; Ganxian cave (362 ± 78 ka - 168.9 ± 2.4 ka; Liang et al., 2022) and Wuyun cave (279–76 ka; Rink et al., 2008) of Middle Pleistocene age; and Luna cave (127–70 ka; Bae et al., 2014) and Baolai cave (54–24 ka; Fan et al., 2022a) from the Late Pleistocene (Fig. 1). Although the biochronological sequence has been established, the evolutionary pattern of these faunas still needs to be described for the region.

In the nearby Chongzuo region, the evolutionary history of Early Pleistocene faunas has been largely discussed (Jin et al., 2014; Wang et al., 2014c, 2017b), with a particular focus on the extinction of some archaic taxa, especially *Gigantopithecus* (Zhang and Harrison, 2017). These Early Pleistocene mammalian faunas, defined as the "*Gigantopithecus-Sinomastodon*" faunal unit, persisted from Baikong Cave (~2.2 Ma) (Sun et al., 2017) to Hejiang Cave (400–320 ka) (Zhang et al., 2016) in the Middle Pleistocene. The occurrence of new taxa in some lineages (e.g. *Stegodon huananensis - Stegodon orientalis*, and *Ailuropoda wulingshanensis - Ailuropoda baconi*), along with a higher percentage of extant taxa *versus* extinct taxa, were together regarded as characteristic of the Middle Pleistocene *Ailuropoda-Stegodon* faunal unit (Wang et al., 2017b). In contrast, the transition from the Middle to Late Pleistocene still lacks attention with few reported fossil sites (Jin et al., 2009) or sites with debated ages (Ge et al., 2020).

In this study, we describe a new faunal assemblage from the Zhongshan cave in the Bubing Basin, that dates to the late Middle Pleistocene. The composition of the Zhongshan fauna is then compared with the Early to Late Pleistocene faunas from this region, Chuifeng cave (Liao et al., 2023), Mohui cave (Wang et al., 2014a), Ganxian cave (Liang et al., 2022), Luna cave (Bae et al., 2014), and Baolai cave (Fan et al., 2022a), and with two Middle Pleistocene faunas from the Indochinese Peninsula in Southeast Asia: Tham Wiman Nakin in Thailand (>169 ka; Suraprasit et al., 2020) and Coc Muoi cave in northern Vietnam (148–117 ka; Bacon et al., 2018). We used the proportions of extinct taxa *versus* extant taxa, and the proportions of taxa that the faunal assemblages shared at the species or genus level, by period and by region, to place the Zhongshan fauna within a biochronological framework and to identify major faunal changes through the Pleistocene.

In addition, we compared the evolutionary faunal pattern based on known palaeontological records between the Bubing Basin and the Chongzuo region at the transition from the Middle to Late Pleistocene to highlight evolutionary dynamics of megafaunas in southern China.

2. Geological context and chronology

The Zhongshan site (23°34′19.956″N, 107°0′31.752″E) is located in the southeastern part of the Bubing Basin, Guangxi, southern China (Fig. 1). The entrance of Zhongshan is a rock shelter with a gentle slope, at an elevation of ~150 m above sea level (asl) and ~10 m above the alluvial plain. The altitude of this cave is ~75 m lower than that of Chuifeng cave (~225 m asl) situated at the top of a nearby peak (Fig. 1). Following the entrance that faces west, stretches a narrow corridor ~60 m long to a large terminal chamber. The fossiliferous deposits were only found in this U-shaped chamber (Fig. 2). The deposits were divided into two units based on the stratigraphy (Tian et al., 2020). The upper unit, dated to ~8.2 ka, is thin with a stalagmite on the top (L1) and with layers of flowstones and charcoal (L2). Most of this unit has been destroyed by local villagers. However, stone artifacts (most likely Holocene) have been found in the remaining profile (Tian et al., 2020). The lower unit, relatively well-preserved, is composed of several layers of sandy clay mixed with limestone breccias about 1.5 m thick (Fig. 2), from the top to the bottom:

L1 Grey-brown stalagmite, ~20 cm;
L2 Light-brown layered flowstones and charcoal, ~5 cm;
———————— Depositional unconformity————————
L3 Light-brown sandy soil with fragmentary flowstones, ~20 cm;
L4 Light-brown sandy clay containing rich mammalian fossils, ~45 cm;
L5 Dark-brown sandy clay with few fossil remains, > 80 cm.

The lower unit yielded numerous mammalian fossils, mainly isolated teeth, excavated in 2006, 2010 and 2019. There is a depositional unconformity between L2 and L3, that represents a long geochronological gap, between the Middle Pleistocene and Holocene (Tian et al., 2020). All mammalian remains in this study were excavated from L4, L5 and also collected from the disturbed deposits of both L4 and L5. From the study of Liang et al. (2024), a total of 9 U-series dating samples were collected from L4, L5 and the boundary of these two layers. The results,

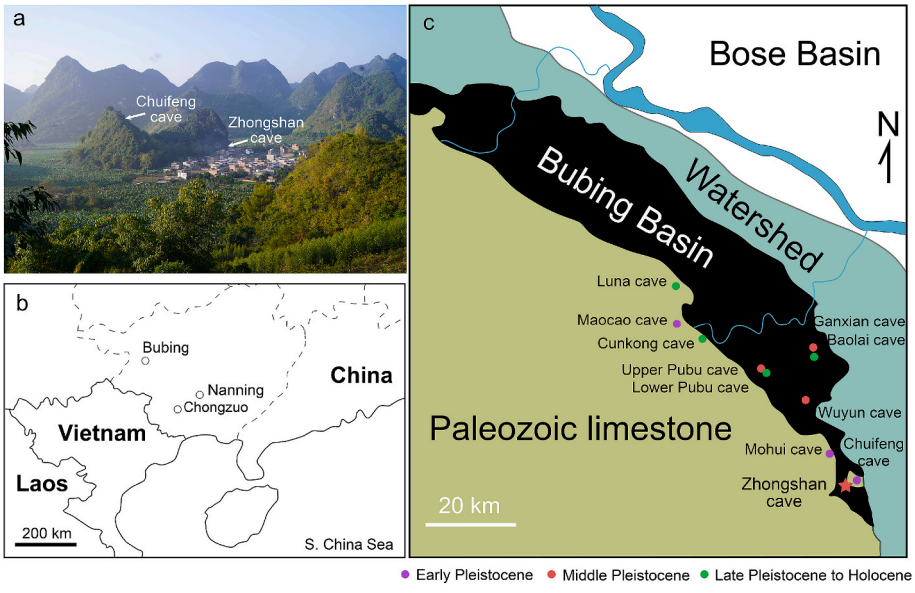

Fig. 1. The cave sites in the Bubing Basin and the location of the Zhongshan cave. (a) The landscape around the Zhongshan cave; (b) Location of the Bubing Basin and the Chongzuo region in southern China; (c) Map showing the distribution of caves in the Bubing Basin. The red star refers to the Zhongshan cave studied here.

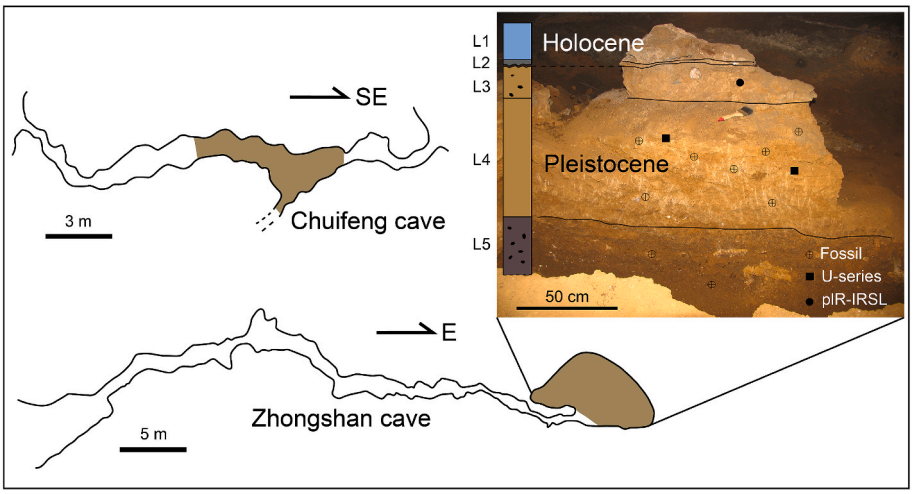

Fig. 2. Plans of the Chuifeng cave and Zhongshan cave and stratigraphy of the fossil-bearing sediments in the Zhongshan cave (see the text for the description of layers).

from 124.947 ± 1.675 to 151.442 ± 1.423 ka, are consistent and indicate a relatively short period of accumulation. These dating results from U-series methods provide the youngest ages for the deposit. Based on coupled electron spin resonance and uranium-series (ESR/U-series) dating methods, a rhinoceros tooth from L4 has been dated to 184 ± 16 ka. The faunal assemblage can be comfortably placed in Marine Isotope Stage (MIS) 6 (191–130 ka).

3. Material and methods

3.1. Material

Most mammalian teeth collected in Zhongshan during the 2006 and 2010 excavations are curated in the Natural History Museum of Guangxi in Nanning. Additional fossil material coming from the 2019 excavation has also been included in the study (SI-Table 1). Due to a complex depositional history, that included gnawing activities of porcupines and fluvial transport and deposition of remains into these karst caves, mostly only isolated teeth and petrosal bones, which represent the hardest and most dense biological tissues, have been preserved. Because all of the osseous fossils were unidentifiable fragmentary pieces, our taxonomic analysis focused on the abundant teeth.

3.2. Methods

Dimensions of the tooth crown, i.e., the maximum length (L) from the mesial to the distal side and the maximum width (W) from the buccal to the lingual side, were measured with a digital caliper. Based on size and morphology, the specimens were identified at the species level when possible. In the following descriptions, lower teeth are represented by lowercase letters (i/c/p/m) and upper teeth by capital letters (I/C/P/M). The number of identified specimens (NISP) and the minimum number of individuals (MNI) based on the most frequent dental element, were calculated for each taxon. We relied on standard dental nomenclatures from published sources: Primates (Swindler, 2002; Takai et al., 2014), Hystricidae (van Weers, 1990; Tong, 2008), Proboscidea (Maglio, 1973; Roth and Shoshani, 1988), Ursidae (Jiangzuo et al., 2019; Pan et al., 2023; Hu et al., 2023), Mustelidae (Jiangzuo et al., 2018a, 2018b; Chen et al., 2023), other Carnivora (Pan et al., 2023; Suraprasit et al., 2020), Rhinocerotidae (Yan et al., 2014), Suidae (van der Made, 1996; Fujita et al., 2000; Chen, 2004), Cervidae (Bärmann and Rössner, 2011; Zhang et al., 2018), other Artiodactyla (Colbert and Hooijer, 1953; Bärmann and Rössner, 2011; Suraprasit et al., 2016).

We examined the number and percentage of extinct taxa *versus* extant taxa, and shared taxa between faunal assemblages by biochronological sequence and across regions (see the faunal lists in SI-Table 2), either at the genus or species level. Our comparisons focused on the taxonomic composition of the Zhongshan fauna in relation to other faunas within the same Basin across three periods, Early Pleistocene, late Middle Pleistocene, and Late Pleistocene, in order to identify evolutionary changes. Furthermore, we investigated two late Middle Pleistocene faunas from Southeast Asia to understand shifts in the distribution of these mammalian taxa.

4. Results

4.1. Description of the zhongshan faunal assemblage

4.1.1. Primates

4.1.1.1. Cercopithecidae. Most specimens (n = 78) are assigned to an undetermined macaque. The upper canines generally display a marked groove on the mesial side. Upper molars are low crowned with a shallow median buccal notch. The M3s exhibit more reduced distal lobes, some with a distoconulus. The lower molars are bilophodont and rectangular in shape, and the m3 displays a hypoconulid positioned buccally (Fig. 3-7). Although slightly larger than some other fossil specimens (Fan et al., 2022b; Suraprasit et al., 2020; Bacon et al., 2008), the features are similar to those of living macaques (Swindler, 2002). Due to the difficulty in identifying the different species, we attribute these teeth to *Macaca* sp. A set of incisors (n = 9) of different sizes are assigned to Cercopithecidae indet.

4.1.1.2. Colobinae. Twenty-six teeth have sharp cusps and a deep median lingual notch, and the mesial and distal lophes are continuous and parallel in the upper molars (Fig. 3) (Takai et al., 2014). Nineteen teeth can be attributed to the large-sized *Rhinopithecus* sp., and the remaining (n = 7) to the smaller *Pygathrix* sp. Compared to *Rhinopithecus*, the molars of *Pygathrix* have sharper ridges and cusps, m3s are nearly rectangular and the hypoconulid is clearly distinct (Fig. 3-10).

4.1.1.3. Hylobatidae. Only two teeth (one upper molar and one lower canine) are attributed to *Hylobates* sp. The crown of the highly worn M1 (L/W = 6.2/7.15 mm) is square (Fig. 3-11). An oblique ridge extends from the protocone to the metacone.

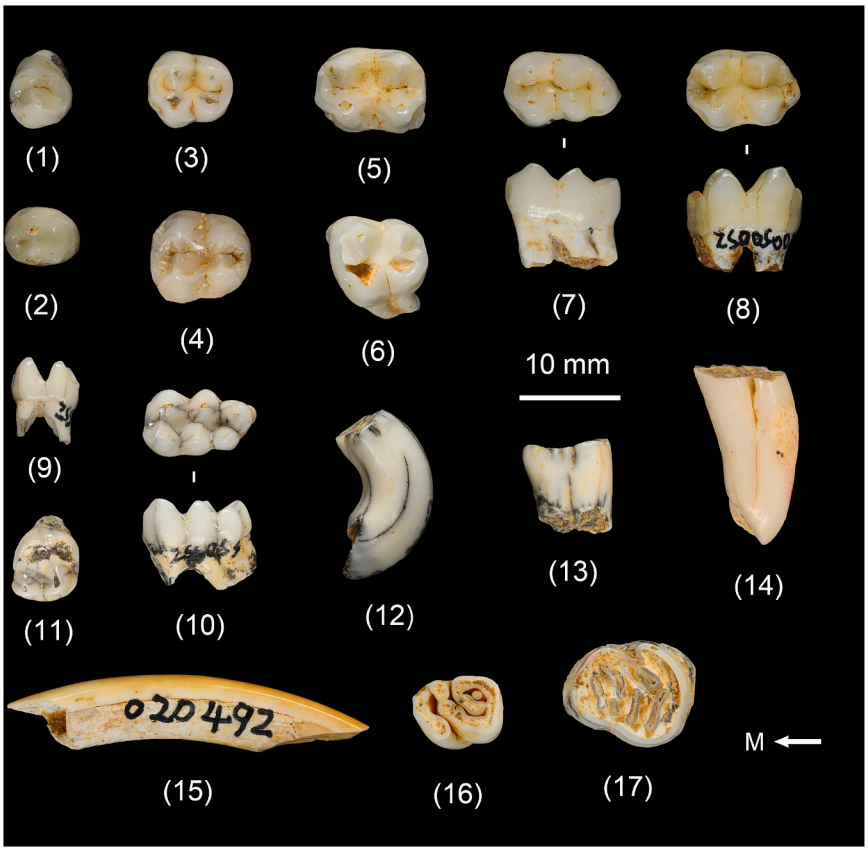

Fig. 3. Primates and porcupines from the Zhongshan cave. *Macaca* sp. (1) right P4, ZSS050; (2) right p4, ZS009002; (3) left M2, ZS001002; (4) right M3, ZSS018; (5) left m2, ZSS066; (6) left M3, ZS003004; (7) left m3, ZS001003. *Rhinopithecus* sp. (8) left m3, ZS005002. *Pygathrix* sp. (9) left m1/2, ZS071; (10) right m3, ZSS053. *Hylobates* sp. (11) right M1, ZSS070. *Hystrix subcristata* (12) left M3, ZS006005; (13) right dp4, ZS003005; (14) left m1/2, ZS019628; (15) right i1, ZS020492; (16) left M1/2, ZS021119. *Hystrix magna* (17) right p4, ZS020495. (1)–(6), (11), (16) and (17), in occlusal view. (7), (8) and (10), in occlusal and lingual view. (9) and (13), in lingual view. (12) and (15) in mesial view. (14), in buccal view. M = Mesial (for occlusal views).

4.1.1.4. Ponginae. One hundred and seventeen teeth belong to *Pongo devosi*, a taxon first described by Schwartz et al. (1995). Their dimensions are significantly smaller than the teeth of *P. weidenreichi* from Ganxian cave and other Pleistocene sites in southern China. The morphological traits are described in Liang et al. (2024).

4.1.2. Rodentia

4.1.2.1. Hystricidae. All rodent specimens (except one small incisor) were assigned to large porcupines (Fig. 3). The assemblage consists of 17 milk teeth and 325 permanent teeth. Twenty permanent premolars and molars belong to *Hystrix magna,* based on their relatively larger size, and thicker enamel (Fig. 3-17; SI-Table 1). The other specimens have the dental pattern of *Hystrix subcristata*, a taxon commonly found in southern China. The deciduous teeth are characterized by lower crowns (Fig. 3-13). The size range of premolars and molars overlaps with that of *H. subcristata* from Tianyuan Cave, Yixiantian Cave and Mocun Cave (Tong, 2005a; Pan, 2021; Fan et al., 2022b).

4.1.3. Carnivora

4.1.3.1. Mustelidae. Eighty-two specimens, mostly isolated teeth, were attributed to four taxa (*Martes flavigula, Lutrogale* sp., *Arctonyx collaris*, *Meles* cf. *leucurus*) based on morphology and dimensions (Fig. 4) (SI-Table 1).

Martes is represented by one incomplete left mandible (p2 to m1, Fig. 4-10). The premolars all show a strong main cusp and an enlarged distal ridge. The m1 shows a relatively elongated paraconid. A distinct fovea appears between the paraconid and the metaconid. The hypoconid, the lowest of the buccal cusps, surrounds the talonid without a separated hypoconulid. The dental pattern of the Zhongshan teeth is close to that of *Martes flavigula* from Yangjiawan Cave 2 and Tham Wiman Nakin (Jiangzuo et al., 2018a; Suraprasit et al., 2020). However, the dimensions are in the range of the extant taxon and smaller than those of Yangjiawan Cave 2.

Only one M1 (Fig. 4-8) has been assigned to *Lutrogale* sp. The crown is rhomboid in shape with a developed cingulum. The protocone is more posterior than the paracone. The specimen shows features of Lutrinae that resemble modern *Lutrogale perspicillata* (Hwang and Larivière, 2005). There are three genera of otters living in China: the large *L. perspicillata*, the medium-sized *Lutra Lutra*, and the small *Amblonyx cinerea* (Chen et al., 2023). The size of the Zhongshan specimen is larger than that of *Lutra* from Jianshi and modern *Lutra* (Zheng, 2004; Ansorge and Stubbe, 1995). Thus, we assigned the specimen to *Lutrogale* sp.

The other teeth are M1/m1 of *Arctonyx*. The size of these Zhongshan specimens falls within the ranges of extant and fossil *A. collaris* (Pan et al., 2023; Helgen et al., 2008). A second badger is represented by jugale teeth (2P4, 16M1 and 2m1). In general, the dimensions of *Meles* are relatively smaller. The position of the midpoint of the inner cusps lies around the anterior margin of the paracone on the P4s (Fig. 4-2). The *Meles* M1s differ from those of *Arctonyx* by the following characteristics: a metastyle less developed or absent, a distinct labial incision between the metacone and metaconule, and a smooth postero-buccal edge (Fig. 4-1). Although the m1s are highly worn, we can observe that the paraconid is not reduced. A notch between the paraconid and the protoconid is also present. According to the data from Jiangzuo et al. (2018b), the m1s of *Meles* have wider talonids than *Arctonyx*. Based on size, we assigned these specimens to *Meles* cf. *leucurus.*

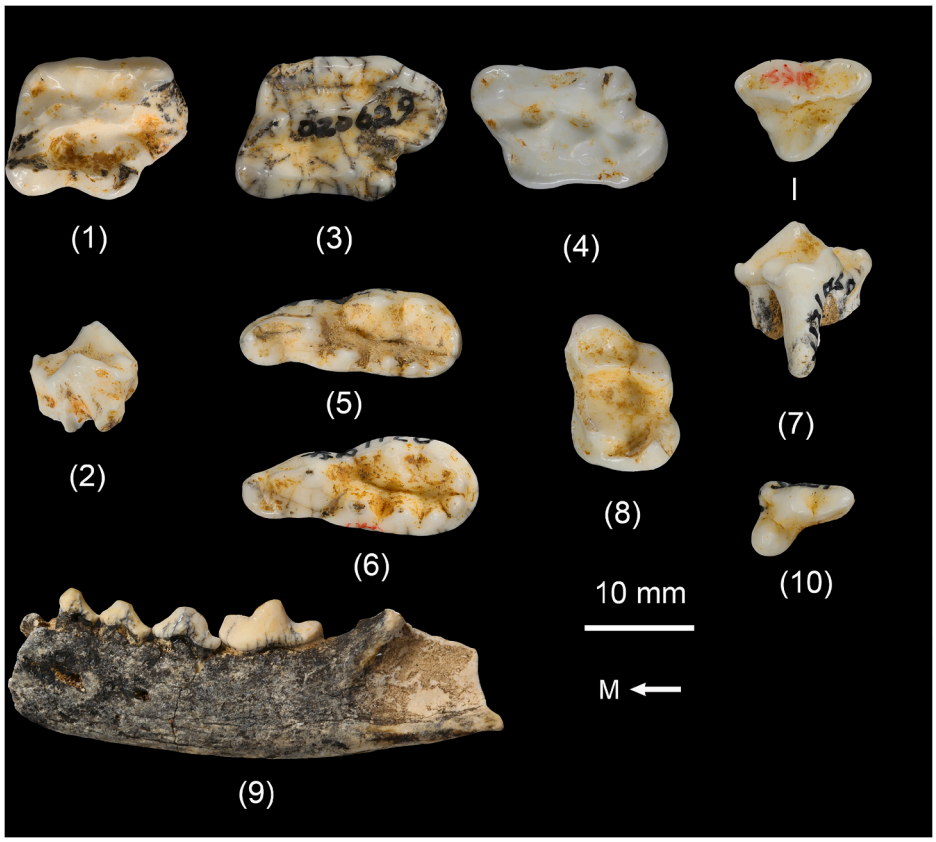

Fig. 4. Small carnivora from the Zhongshan cave. *Meles* cf. *leucurus* (1) right M1, ZS020148; (2) right P4, ZS020502. *Arctonyx collaris* (3) right M1, ZS020629; (4) left M1, ZS011006; (5) right m1, ZS020657; (6) right m1, ZS021194; (7) right P4, ZS020154. *Lutrogale* sp. (8) left M1, ZS020645. *Martes flavigula* (9) left mandible fragment, ZS020698. Viverridae indet. (10) left P4, ZS005001. (1), (3), (4), (5), (6), (8) and (10), in occlusal view. (2), in lingual view. (7), in occlusal and lingual view. (9), in buccal view. M = Mesial (for occlusal views).

4.1.3.2. Canidae. Seven specimens show the canid morphology (Fig. 5). One P4 (Fig. 5-16) resembles the pattern of *Canis*: no reduction of the protocone; the anterior rim of the protocone is located slightly anterior to that of the paracone; and a distinct depression lies on the contour between the paracone and the protocone. The p3/p4 has a small posterior accessory cusp with no developed anterior or second posterior accessory cusp (Fig. 5-17). Moreover, its small size is close to that of *Canis mosbachensis variabilis* from Zhoukoudian Locality 1 (Jiangzuo et al., 2018c). Based on only two teeth, we propose an attribution to *Canis* sp.

Two P4s assigned to the genus *Cuon* display a weakly-developed protocone which lies posterior to the anterior rim of the paracone. The metaconule is absent on the M2 and the inner lobe is oriented posteriorly (Fig. 5-12). The paracone is well developed. One complete p4 has a clear distal cingulum comparable in size with the metastylid. The parastylid is also present. These characteristics conform to *Cuon alpinus* (Jiangzuo, 2021).

4.1.3.3. Hyaenidae. Only one p2 was recovered from Zhongshan (Fig. 5-11). This specimen belongs to a large carnivore, but is different from the teeth of *Panthera*. The dental pattern and dimensions are close to those of Mocun Cave and Ganxian Cave specimens that have been assigned to *Crocuta ultima* (Fan et al., 2022b; Liang et al., 2022). We cautiously assigned this p2 to *Crocuta* cf. *ultima*.

4.1.3.4. Viverridae. Viverridae are represented by two P4s. They exhibit blunt cusps unlike *Viverra*. The P4 (Fig. 4-9) has a well-developed protocone, and a small notch between the paracone and the protocone. These specimens are attributed to Viverridae indet.

4.1.3.5. Felidae. One canine, two P4s, one p4 and two m1s are attributed to the tiger, *Panthera tigris*. The P4s show a well-developed parastyle, a blade (formed by the metastyle and the metacone), and, on the lingual side, a small protocone, as in extant *P. tigris* (Fig. 5-13). Only one smaller P4 was assigned to the leopard, *Panthera* cf. *pardus*. The buccal margin between the parastyle and the main cusp shows a marked notch. One P3 (Fig. 5-18), two P4s and one m1 (Fig. 5-19) are attributed to *Neofelis nebulosa* based on their dimensions. The P4s differ from those of *Catopuma* by the presence of a ridge between the paracone and the protocone and the curved buccal margin. The smaller felid *Felis* cf. *chaus* is represented by one P4. The protocone is larger than the parastyle and anterior to the mesial rim of the parastyle. The lingual side shows a strong cingulum. The dimensions of this specimen fall within those of the sample from Yixiantian cave (Pan et al., 2023).

4.1.3.6. Ursidae. In relation to ursids, 56 teeth clearly show the features of *Ursus thibetanus*. The other specimens (2 P4s, 2 M1s, 1 M2, 2 m1s, 2 m2s, 1 m3) conform to the morphology and dimensions of the smaller species *Helarctos malayanus*. Besides a size difference, the P4s of *H. malayanus* display oval outlines. The hypocone is reduced. In both species, the M1s have a rectangular outline and a well-developed paracone and metacone. However, the parastyle is more distinct in *U. thibetanus*, and the hypocone is oriented buccally. The mesostyle is usually absent in *H. malayanus* and m1/m2 (Fig. 5-5) have a simple occlusal pattern and a smaller length. The m1 displays a metaconid with no posterior ridge (Fig. 5-6). Teeth dimensions are comparable to those of the two species from Yixiantian and Tham Wiman Nakin caves (Pan, 2021; Suraprasit et al., 2020).

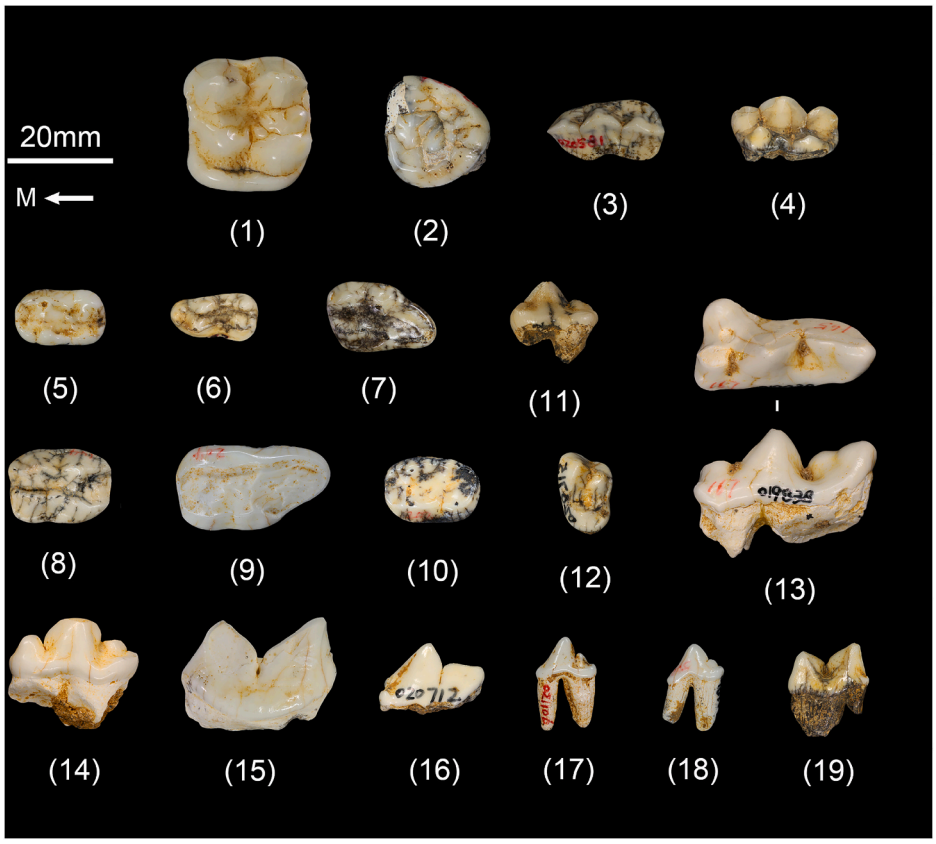

Fig. 5. Large carnivora from the Zhongshan cave. *Ailuropoda baconi* (1) left M1, ZS020589; (2) left m3, ZS020586; (3) left p4, ZS020581; (4) left P3, ZS020580. *Helarctos malayanus* (5) right m2, ZS020612; (6) left m1, ZS020583; (7) left M2, ZS020643. *Ursus thibetanus* (8) left M1, ZS021117; (9) right M2, ZS020164; (10) left m3, ZS020165. *Crocuta* cf. *ultima* (11) right p2, ZS020620. *Cuon alpinus* (12) left M2, ZS020715. *Panthera tigris* (13) right P4, ZS019838; (14) right p4, ZS019837; (15) left m1, ZS020719. *Canis* sp. (16) left P4, ZS020712; (17) left p3/4, ZS021106. *Neofelis nebulosa* (18) right P3, ZS019668; (19) right m1, ZS020711. (1)–(3), (5)–(7) and (8)–(12), in occlusal view. (4), (11), (14), (16), (18) and (19), in lingual view. (13), in occlusal and buccal view. (15) and (17), in buccal view. M = Mesial (for occlusal views).

4.1.3.7. Ailuropodinae. Fifteen specimens were attributed to *Ailuropoda melanoleuca baconi* (1 C, 4 P3s, 3 M1s, 1 M2, 1 M, 1 p3, 2 p4s, 1 m3). The upper premolars display three well-developed cusps in the same line, and two lower rounded cusps on the lingual side. The molars have complicated occlusal patterns with small ridges as well as cusps. The only complete M1 shows a square outline (Fig. 5-1). Between the main cusps on the lingual and buccal sides, we can observe several well-developed ridges and a complex entmetaconule. The cingulum surrounding the cusps is extremely marked on the lingual side, forming a valley with the protocone and the hypocone. The m3 presents a subtriangular shape (Fig. 5-2). The occlusal surface is covered by numerous tubercles and ridges. These features and the dimensions of the teeth are comparable to those of the *A. m. baconi* specimens from Yangjiawan Cave 2 (Jiangzuo et al., 2018a).

4.1.3.8. Carnivora indet. Eleven incisors and canines could only be identified as carnivores, but not to a lower taxonomic level.

4.1.4. Proboscidea

4.1.4.1. Stegodontidae. Proboscidean fossils are only represented by tooth fragments. The parameters for species identification are therefore impossible to estimate. Several isolated dental lophes display a low-crowned appearance with thick enamel. We assigned the specimens to *Stegodon* sp.

4.1.4.2. Elephantidae. The other fragments showing a high crown and thinner enamel have been attributed to *Elephas* sp. Only one incomplete lower milk tooth has three aligned lamellae covered with cement. The residual width is 44.45 mm.

4.1.5. Perissodactyla

4.1.5.1. Rhinocerotidae. One fragmentary upper premolar, three lower premolars and six milk teeth of rhinoceros have been recovered at Zhongshan (SI-Table 1). The heavily worn DP1 has a small paracone fold with a median valley and a shallower postfossette. The paraconid of the dp1s is elongated from the protoconids (Fig. 6-3) and the metaconid is absent. The ectoflexid is present on the dp2s (Fig. 6-4). On the dp2s, an anterior valley is opened lingually and a shallow posterior fossette is present. The pillars of the upper premolar are damaged. The crochet is well developed but still separated from the protoloph. The crista is absent. The paraloph and metaloph are nearly parallel. This upper premolar shows a median valley deeper than the post fossette (a character in which it differs from the M1), and a slightly more distinct protocone constriction compared to the P3 (Fig. 6-2). Therefore, we attribute this tooth to a P4. The p2 is heavily worn and the trigonid is fused. It is smaller than the p3s. Two lower premolars have a relatively less marked paralophid in comparison with the p4 and the molars. The trigonid basin is only visible in unworn or slightly worn premolars. These characteristics resemble those of the p3s. Based on the observed morphological features and small dimensions of the p3s and deciduous teeth, which fall within the size range of *Rhinoceros sondaicus* from Coc Muoi Cave (Bacon et al., 2018), we are inclined to refer these teeth to *R. sondaicus*.

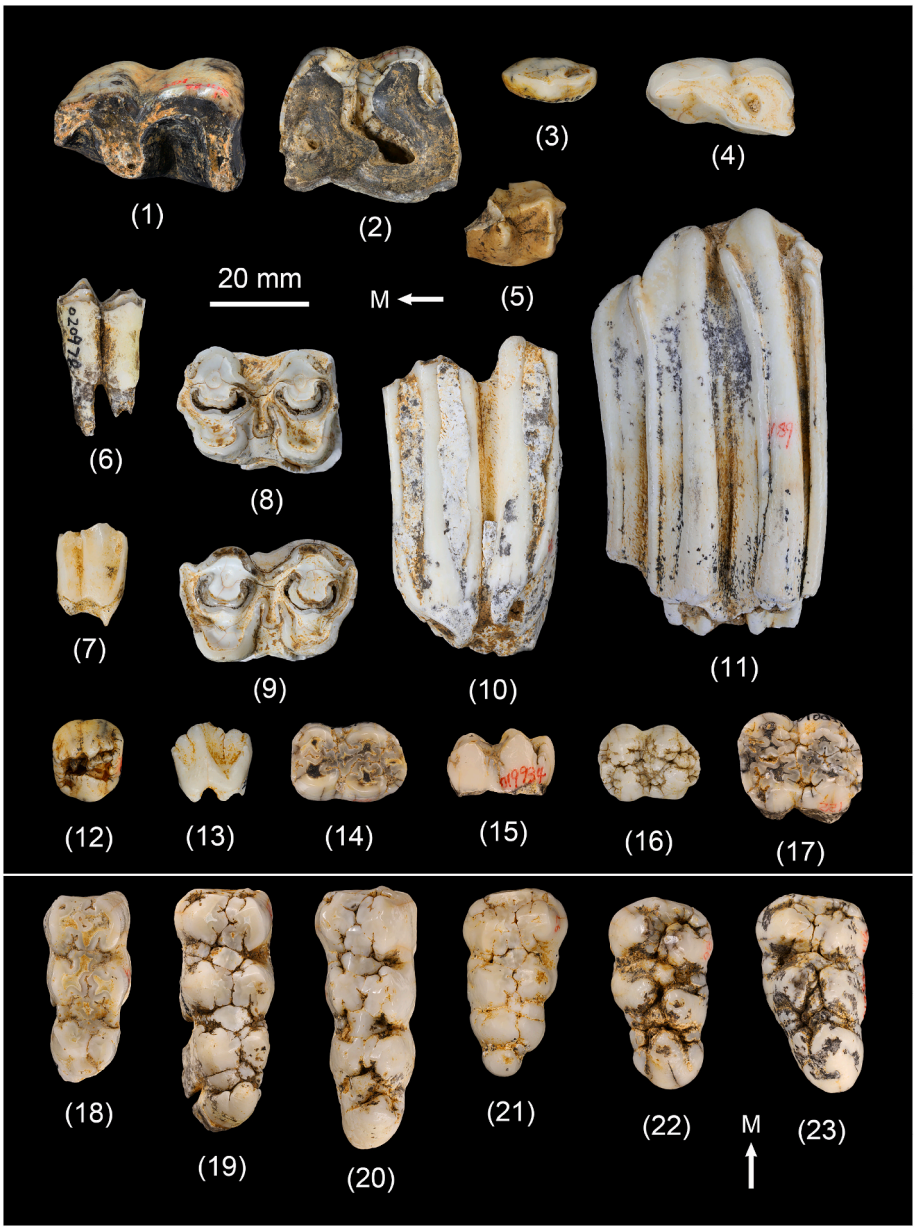

Fig. 6. Perissodactyla and Artiodactyla from the Zhongshan cave. *Rhinoceros sondaicus* (1) right p3, ZS021115; (2) left P4, ZS021116; (3) left dp1, ZSD04015; (4) right dp2, ZSD04032. *Tapirus* sp. (5) right p2, ZSD05001. *Capricornis sumatraensis* (6) left m1/2, ZS020978; (7) left p4, ZS020505. *Bubalus arnee* (8) left m1, ZS021131; (9) left m2, ZS021130; (10) left M1, ZS021109; (11) left m3, ZS020176. *Sus scrofa* (12) left P4, ZS020244; (13) left p4, ZSD04007; (14) right m2, ZS019932; (15) left m2, ZS019934; (16) left M1, ZS019598; (17) left M2, ZS019931; (18) left m3, ZS019589; (19) left m3, ZS019583; (20) left m3, ZS020661; (21) left M3, ZS019587; (22) right M3, ZS020662; (23) right M3, ZS019933. (1)–(5), (8), (9), (12), (14) and (16)–(23), in occlusal view. (6), (10), (13) and (15), in buccal view. (7) and (11), in lingual view. M = Mesial (for occlusal views).

4.1.5.2. Tapiridae. One fragmentary upper molar and one incomplete p2 were cautiously assigned to *Tapirus* sp. The paracristid and the protoconid are missing on the p2 and there is a notch between the hypoconid and the entoconid (Fig. 6-5). Both specimens fall within the size range of the extinct *Tapirus sinensis* and the modern *T. indicus* (Zheng, 2004; Bacon et al., 2018).

4.1.6. Artiodactyla

4.1.6.1. Suidae. Numerous isolated teeth (702 permanent and 23 deciduous teeth) were assigned to *Sus scrofa*. They are considerably variable in size (SI-Table 1). One incomplete lower canine without root, likely a male individual, displays the scrofic type, i.e. the labial face of the crown is the narrowest (Fujita et al., 2000). The M3/m3 are the most useful teeth in separating the different suid species. Chen (2004) revised the diagnostic features of *S. peii*: molars with high crowns; the third lobe of the M3 composed of large cusps; and a small and simple talonid on the m3 and the fourth lobe is absent (also see Sun et al., 2021). However, the m3s of *S. scrofa* from the Dadiwan Neolithic site also show great variability and some display a similar pattern, which makes it difficult to discriminate *S. peii* from *S. scrofa*. Within the Zhongshan suid assemblage, six M3s display one large cusp as the third lobe (Fig. 6-23), whereas five M3s developed a third lobe with several additional small cusps (Fig. 6-21). On four out of the six m3s, the fourth lobe varies in size with an increasing number of heptaconid cusps (Fig. 6-19, 6-20). Based on the characteristics of the male lower canine, we attribute the Zhongshan specimens to *S. scrofa*.

4.1.6.2. Cervidae. They represent the largest proportions of teeth in the Zhongshan assemblage. They belong to four species that differ in size: *Rusa unicolor*; *Cervus nippon*; *Muntiacus muntjac*; and *Muntiacus reevesi*.

A total of 639 teeth have been assigned to the largest species *R. unicolor*. The enamel is thick and wrinkled. On the lingual side of the P2s and P3s two distinct lobes are present, protocone and hypocone (Fig. 7-4), whereas on the P4s only a weak (or absent) groove appears between the cusps. Developed bilobate or trilobate entostyles are present on the lingual side of the upper molars. Styles, crista and cingulum are also well-developed. The width of the posterior lobe decreases from M1 to M3 (Fig. 7-25). The majority of the p4s are molarized due to the fusion of the metaconid with the paraconid (closure of the second valley) as well as the fusion of the entoconid with the entostylid (closure of the posterior valley) (Fig. 7). The lower molars lack a *Palaeomeryx* fold. A well-marked ectostylid is also present. The deciduous teeth, though composed of thinner enamel, are well-preserved in the Zhongshan fossil assemblage. The dp3s can be distinguished by salient and elongated posterior wings of the paraconid and the metaconid. Most dp4s have three similar lobes, but in a few specimens, the third lobe appears more distinct. The size of the milk teeth is similar to those of Duoi U'Oi and Coc Muoi (Bacon et al., 2008, 2015).

One hundred and thirteen medium-sized teeth are assigned to *C. nippon*, with a comparable morphological pattern as that observed in the specimens from the Yangjiawan and Fuyan caves (Zhang et al., 2018). In addition to a smaller size, *C. nippon* differs from *R. unicolor* primarily by upper molars with a columned entostyle and a thinner cingulum (Fig. 7-14). The *C. nippon* teeth have a less angular outline compared to the teeth of the larger species.

Muntiacus muntjak is represented by 6 deciduous and 650 permanent teeth. The protocone of the P2s is separated from the hypocone and the metastyle is more salient than the parastyle. The position of the paracone is more anterior in the P3s than in the P4s (Fig. 7-11). The anterior lobe of the upper molars presents stronger styles and crista. The hypocone is oblique in the M2/M3. Concerning the lower premolars, the parastylid is absent on the p2s (Fig. 7-6). On the p3s, a developed paraconid is fused with the parastylid, whereas the metaconid is clearly distinct (Fig. 7-7). The m1s and m2s have two similar lobes, and it is difficult to distinguish the m1 from the m2 (Fig. 7-9). The m3s display three lobes with the third one composed of an entoconulid and a hypoconulid. Their dimensions largely overlap with those of specimens from Mocun Cave (Fan et al., 2022b), Duoi U'Oi Cave (Bacon et al., 2008), and extant taxa (Suraprasit et al., 2020). The upper milk teeth are identified as DP4s by the more developed hypocone and reduced metastyle and metacone. The lower dp4 presents a developed hypoconid and two ectostylids between the three lobes (Fig. 7-3).

Fifteen significantly smaller dental specimens are attributed to *M. reevesi* (Fig. 7-1 and 7-2). Besides the size, these teeth also show sharper styles/stylids, cusps/cuspids, but small entostyles. The size of these Zhongshan specimens falls within the range of the Ganxian and Mocun *M. reevesi* (Liang et al., 2022; Fan et al., 2022b) (Fig. 8).

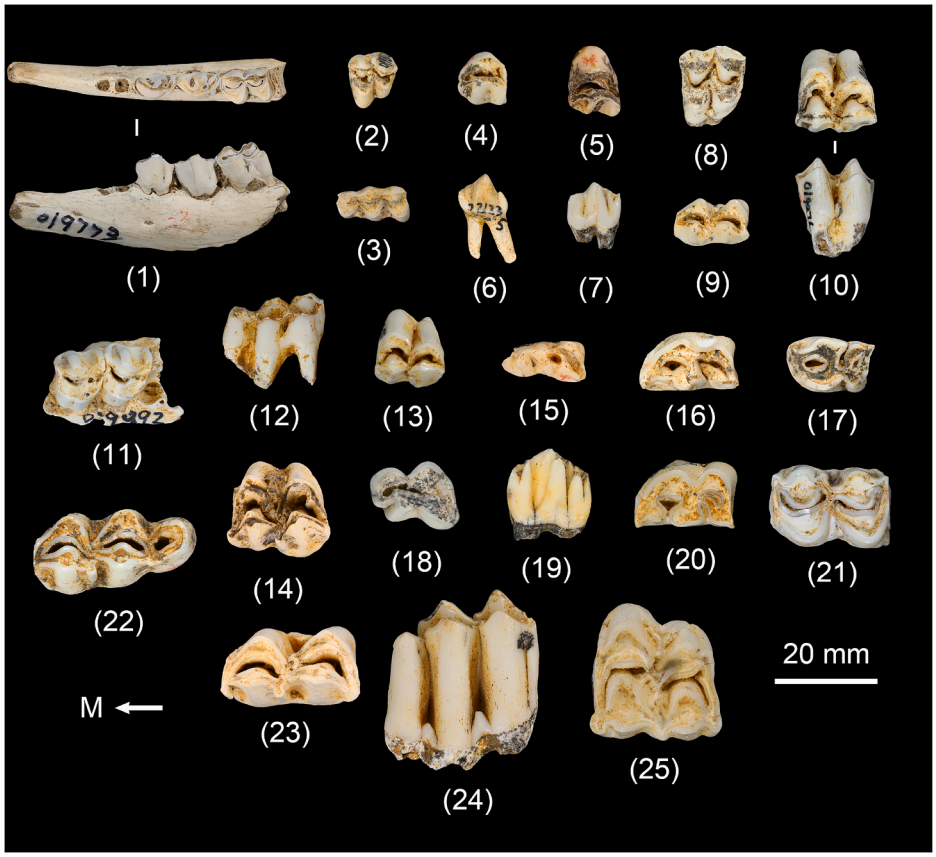

Fig. 7. Cervidae of the Zhongshan cave. *Muntiacus reevesi* (1) left mandible fragment, ZS019773; (2) left M3, ZS019917. *Muntiacus muntjak* (3) left dp4, ZS021144; (4) right P2, ZS021232; (5) right P3, ZS021210; (6) left p2, ZS021235; (7) right p3, ZS021231; (8) left M1/2, ZS021224; (9) right m1/2, ZS021220; (10) right M1/2, ZS019876; (11) left maxillary fragment, ZS019992; (12) right m3, ZS020985; (13) right M3, ZS020983. *Cervus nippon* (14) right M1/2, ZS021206. *Rusa unicolor* (15) right p3, ZS021204; (16) right p4, ZS021137; (17) left p4, ZS021142; (18) right P2, ZS009001; (19) right p3, ZS021140; (20) right p4, ZS021129; (21) left m1/2, ZS021134; (22) right m3, ZS021133; (23) right m1/2, ZS019852; (24) right m3, ZS020945; (25) right M3, ZS019849. (1), in occlusal and buccal view. (2)–(5), (8), (9), (11), (13)–(18), (20)–(23), in occlusal view. (6), (7) and (19), in lingual view. (10), in occlusal and lingual view. (12) and (24), in buccal view. M = Mesial (for occlusal views).

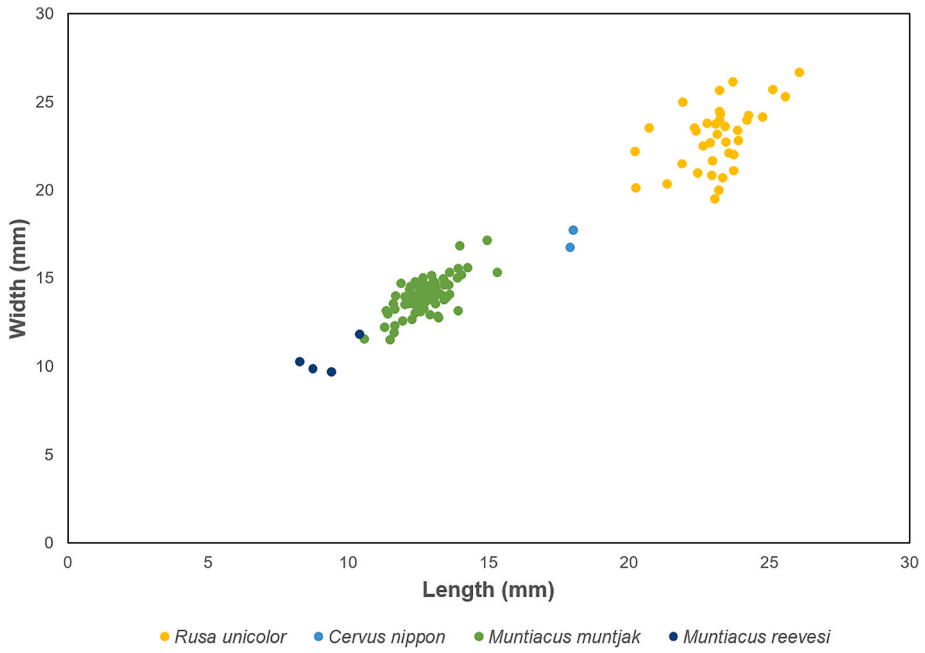

Fig. 8. The size distribution (mesiodistal length and buccolingual width) of M3s in Cervidae (see Supplementary Information for data).

4.1.6.3. Bovidae. A small proportion of specimens belongs to two subfamilies, Bovinae and Caprinae. Overall, the teeth show higher crowns than those of cervids. Among these, 8 upper teeth and 14 lower teeth were assigned to the large-sized caprine *Capricornis sumatraensis*. The p4s are molarized (Fig. 6-7). The lower molars display weak stylids and cristids (Fig. 6-6). The ectostylid is absent. The fossette on the third lobe of the m3 is missing. Furthermore, the dimensions of the Zhongshan specimens largely overlap those of fossil *C. sumatraensis* (Suraprasit et al., 2020; Pan et al., 2023).

Twenty-one teeth are attributed to two species of large bovines (Fig. 5). In a few worn p3s, the posterior inner valley tends to form a closed fossette as in the description of *Bubalus* from Yenchingkou (Colbert and Hooijer, 1953). The m1/m2s possess well-developed metastylids and straight and unbifurcated ectostylids. The m3s (Fig. 6-11) display the morphological pattern of *Bubalus arnee* from Tham Wiman Nakin and Ganxian cave with a strong metastylid and a large fossette on the third lobe (Suraprasit et al., 2020; Liang et al., 2022). The posterior ectostylid is absent on the m3s. We attribute these specimens to *Bubalus arnee*. *Bos gaurus* is represented by one P4, two p4s, one m2 and four m3s. The parastyle of the P4 is compressed. The tooth also displays a more complex fossette than that of *Bubalus*. The p4s exhibit more developed metaconids and constricted postprotocristids. On lower molars, the metastylids are small or absent. The outline of each lobe is more oval. The posterior ectostylid is sometimes missing on the m3s. The dimensions of *Bos* and *Bubalus* of the Zhongshan fossil assemblage are similar. The size of the Zhongshan specimens falls within the range of *Bos gaurus* from Khok Sung (Suraprasit et al., 2016).

4.2. The faunal composition of Zhongshan cave

Thirty-three identified taxa (genus or species level) of six orders (Primates, Rodentia, Carnivora, Proboscidea, Perissodactyla and Artiodactyla) are present in the Zhongshan faunal assemblage (Table 1). Based on the NISP and MNI counts, Artiodactyla (Suidae, Cervidae, Bovidae) is the most abundant group, unlike Perissodactyla (Rhinocerotidae and Tapiridae) and Proboscidea (Elephantidae and Stegodontidae). The composition of the Zhongshan fauna shows a great diversity of Carnivora.

Table 1
List of mammalian taxa from Zhongshan cave.

Taxa	NISP	Proportion	MNI	Proportion
Macaca sp.	79	2.65%	10	3.29%
Rhinopithecus sp.	18	0.60%	3	0.99%
Pygathrix sp.	7	0.24%	2	0.66%
Cercopithecidae indet.	9	0.30%	3	0.99%
Hylobates sp.	2	0.07%	1	0.33%
Pongo sp.	117	3.77%	12	3.95%
Hystrix magna	20	0.67%	4	1.32%
Hystrix subcristata	322	10.83%	23	7.57%
Martes flavigula	1	0.03%	1	0.33%
Lutrogale sp.	1	0.03%	1	0.33%
Arctonyx collaris	62	2.09%	21	6.91%
Meles cf. *leucurus*	21	0.71%	9	2.96%
Canis sp.	2	0.07%	1	0.33%
Cuon alpinus	5	0.17%	2	0.66%
Crocuta cf. *ultima*	1	0.03%	1	0.33%
Viverridae indet.	2	0.07%	1	0.33%
Panthera tigris	6	0.20%	1	0.33%
Panthera cf. *pardus*	1	0.03%	1	0.33%
Neofelis nebulosa	4	0.13%	2	0.66%
Felis cf. *chaus*	1	0.03%	1	0.33%
Ursus thibetanus	56	1.88%	12	3.95%
Helarctos malayanus	10	0.34%	2	0.66%
Ailuropoda baconi	15	0.50%	2	0.66%
Carnivora indet.	11	0.37%	2	0.66%
Stegodon sp.	1	0.03%	1	0.33%
Elephas sp.	1	0.03%	1	0.33%
Rhinoceros sondaicus	10	0.34%	3	0.99%
Tapirus sp.	2	0.07%	1	0.33%
Sus scrofa	725	24.39%	55	18.09%
Rusa unicolor	639	21.49%	57	18.75%
Cervus nippon	113	3.80%	10	3.29%
Muntiacus muntjak	656	22.07%	46	15.13%
Muntiacus reevesi	15	0.50%	3	0.99%
Capricornis sumatraensis	22	0.74%	3	0.99%
Bos gaurus	8	0.27%	4	1.32%
Bubalus arnee	13	0.44%	2	0.66%
Total	**2978**	100.00%	**304**	100.00%

Only five extinct taxa, either genus or species (*Pongo devosi*, *Stegodon* sp., *Crocuta* cf. *ultima*, *Ailuropoda baconi* and *Hystrix magna*), are recorded at Zhongshan. Another three taxa from the Zhongshan Cave (*Bubalus arnee*, *Rhinoceros sondaicus* and *Tapirus* sp.) disappeared from southern China but still survive today in other regions (island or/and mainland) of Southeast Asia.

5. Comparison and discussion

5.1. Mammalian evolution in the Bubing basin in its palaeoenvironmental context

The basin contains a series of Early Pleistocene to Holocene fossil-bearing cave sites, located at varying altitudes that are roughly correlated with the age of the fossiliferous deposits (Wang et al., 2007; Rink et al., 2008). This correlation is supported by the elevation of the Chuifeng cave (Early Pleistocene) situated at ~225 m asl and that of the Zhongshan cave (late Middle Pleistocene) at ~150 m asl on a nearby hill, which clearly represent different evolutionary stages in terms of faunal composition (Fig. 9). The karstic caves at different elevations provide evidence of a geomorphic/tectonic uplift process, while the presence of fluvial terraces on both sides of the Bubing Basin provides evidence of clear fluvial erosion (Zhou et al., 2005; Chen and Wang, 2017; Duringer et al., 2012; Huang et al., 2018). In relation to taphonomic processes, the primary collectors were porcupines based on our observation of gnawing marks on a high percentage of teeth in both Chuifeng and Zhongshan (Table 2).

Our analysis contributes to developing a more robust biochronological framework for the Bubing Basin from the Early Pleistocene (Wang et al., 2014a) to the Late Pleistocene (Fan et al., 2022a). The proportion of extinct taxa, at the species or genus level, decreases significantly from the oldest Chuifeng fauna (64.3%) and Mohui fauna (66.7%) to the youngest Baolai fauna (10.5%). As expected, the extinct taxa are the most frequent in the Early Pleistocene fauna (56.8%, n = 21), whereas extant taxa became predominant from the Middle Pleistocene (73.8%, n = 32). The Late Pleistocene Luna fauna (127–70 ka) still contains 22.2% extinct taxa; however, Luna is based on a small number of taxa and a detailed taxonomic assessment has yet to be undertaken. In this evolutionary framework, the Zhongshan fauna (~184 ka) most resembles the late Middle Pleistocene Ganxian fauna (362–168.9 ka) (Table 3a) with 54.5% shared taxa. The Ganxian fauna has however a higher percentage of extinct taxa (29.6% *vs* 15.2%), in accordance with a likely older age.

Table 2
Compared percentage of specimens showing gnawing marks between the Chuifeng cave and the Zhongshan cave. The percentage is from the total number of observed specimens.

	Chuifeng cave		Zhongshan cave	
	Ungulate	Total fauna	Ungulate	Total fauna
Gnawing marks	345	436	1542	1804
Observed specimens	559	834	2205	2978
Percentage	61.72%	52.28%	69.93%	60.58%

The small number of shared taxa (n = 10) between the Early and Middle Pleistocene implies a greater number of extinction events than between the Middle and Late Pleistocene (n = 16) (Table 3a). However, given the fragmented nature of the record it is difficult to more accurately estimate the rate of these faunal extinctions. This transition phase between the Early and Middle Pleistocene is also evidenced from the early Middle Pleistocene fauna from Yanlidong cave (Yao et al., 2023).

When comparing the late Middle Pleistocene Bubing Basin faunas with those from other peninsular Southeast Asian regions [e.g., Thum Wiman Nakin (>169 ka; Suraprasit et al., 2020) and Coc Muoi (148–117 ka; Bacon et al., 2018)], it is evident that they share a large proportion of taxa at the genus level (79.4% and 84.4%, respectively), indicating the zoogeographical similarity at a broader continental scale (Table 3b). Regionally, within the Bubing Basin area, the Ganxian and Zhongshan faunal assemblages show a high homogeneity as suggested by the greater number of shared taxa both at the species or genus level, than between the Tham Wiman Nakin and Coc Muoi cave faunas. We note also that the proportion of extinct taxa in peninsular Southeast Asia during the late Middle Pleistocene is more similar to that of the Late Pleistocene faunas in the Bubing Basin. In southern China, taxa such as *Hystrix magna*, *Tapirus sinensis* or *Sus xiaozhu*, persisted into the Late Pleistocene likely due to the presence of suitable habitats.

In terms of paleoecology, the great affinity between the late Middle Pleistocene Zhongshan and Ganxian faunas (362–168.9 ka) (Table 3a), suggests similar environments. Previous isotopic studies on large mammal assemblages (e.g. Sun et al., 2021; Stacklyn et al., 2017; Nelson, 2014; Ma et al., 2017) highlighted mixed environments dominated by forests in the Early Pleistocene followed by an increase of more open biomes in southern China during the Middle Pleistocene. On a large time-scale, Louys and Roberts (2020) demonstrated that the forests of the Early Pleistocene had given way in part to more open savannahs by the Middle Pleistocene, which led to the spread of grazers and the

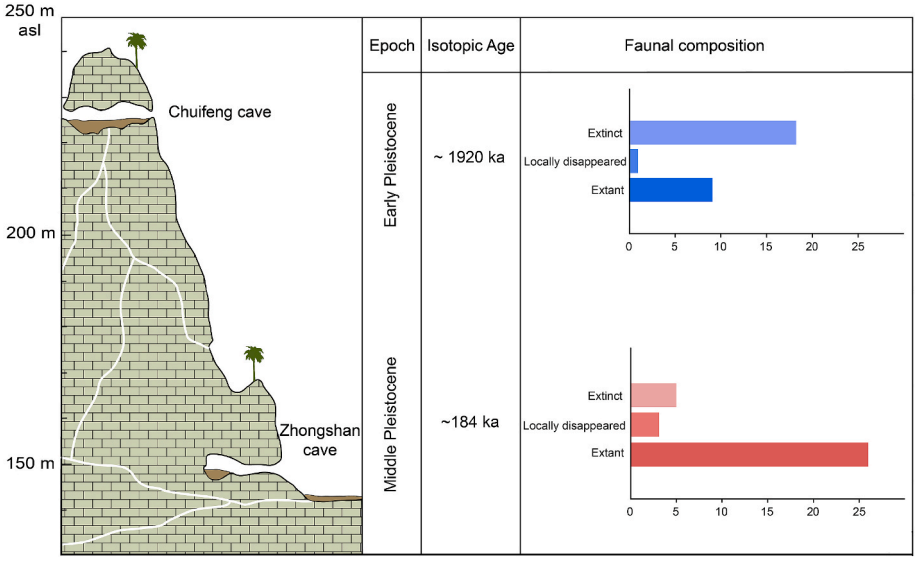

Fig. 9. Compared elevation in the kartic hill, age and faunal composition between the Chuifeng cave and the Zhongshan cave.

Table 3a
Number and proportion of extinct and extant taxa in faunal assemblages (see SI-Table 2). The percentage of shared taxa is estimated by the number of common taxa out of the total number of taxa by site or by period. The "E-M" refers to the Early-Middle Pleistocene; the "M-L" refers to the Middle-Late Pleistocene.

	Chuifeng cave	Mohui cave	Early Pleistocene	Ganxian cave	Zhongshan cave	Middle Pleistocene	Luna cave	Baolai cave	Late Pleistocene
Extinct taxa	18/64.3%	18/66.7%	21/56.8%	8/29.6%	5/15.2%	11/26.2%	2/22.2%	2/10.5%	3/12%
Extant taxa	10/35.7%	9/33.3%	16/43.2%	19/70.4%	28/84.8%	31/73.8%	7/77.8%	17/89.5%	22/88%
Shared taxa	17/60.7%	17/63%	E-M: 10/27%	18/66.7%	18/54.5%	/	3/33.3%	3/15.8%	M-L: 16/64%

Table 3b
Number and proportion of extinct and extant taxa in the late Middle Pleistocene faunas from the Bubing Basin and the peninsular Southeast Asia (see SI-Table 2).

	Ganxian cave	Zhongshan cave	Bubing basin	Tham Wiman Nakin	Coc Muoi cave	Southeast Asia
Extinct taxa	8/29.6%	5/15.2%	11/26.2%	2/7.4%	3/11.5%	4/9.3%
Extant taxa	19/70.4%	28/84.8%	31/73.8%	25/92.6%	23/88.5%	39/90.7%
Shared taxa	18/66.7%	18/54.5%	21/50.0%	10/37%	10/38.5%	21/48.8%
Shared genus	21/84%	21/63.6%	27/79.4%	15/62.5%	15/65.2%	27/84.4%

extinction of browsers. This environmental shift may have led to the noticeable faunal turnover during the Early to Middle Pleistocene transitional period.

Stegodon orientalis was a browsing species in dense forests, that nevertheless indicates the presence over time of canopy forests in the Bubing Basin (Zhang et al., 2016; Ma et al., 2019). Furthermore, along with typical forest-dwelling animals like *Stegodon* sp., *Tapirus* sp., or *Pongo* sp. (orangutans being relatively abundant *versus* macaques at Zhongshan (MNI in Table 1), the Zhongshan fauna also shows diverse and abundant ruminant taxa among Artiodactyla (MNI = 59.22%) *versus* rare large-sized Perissodactyla (MNI = 1.32%) (Table 1; SI-Table 1), which could indicate a diversity of biomes in this ecosystem. Medium-sized cervids are not common in the Bubing Basin, and currently, *Cervus nippon* is only reported in the late Middle Pleistocene Zhongshan cave. With the lack of evidence of hominin impact on the mammalian fauna, the extinction events in the Bubing Basin seems to be due primarily to environmental changes.

5.2. *Evolution of some mammalian lineages in southern China: the Bubing Basin versus the Chongzuo area*

The Bubing Basin and the Chongzuo region slightly further south, are geographically close to each other and both have rich Quaternary fossil records of the *Ailuropoda-Stegodon* faunal complex. The fossil record from Chongzuo is concentrated in the Early to Middle Pleistocene. In contrast, the fossil record from Bubing remains patchy throughout the Pleistocene, with a notable gap between the Early Pleistocene and the late Middle Pleistocene. Based on published data, we can nevertheless attempt to compare the occurrence of some taxa between both regions and infer major events about the decline in megafaunas (Fig. 10).

Five Neogene taxa are present in the Bubing Basin during the Pleistocene; *Sinomastodon*, recorded in both Mohui Cave and Chuifeng Cave, may have disappeared at the end of the Early Pleistocene (Wang et al., 2014b). The extinction of the bunolophodont *Sinomastodon* might have been driven by the change to a cooler and dryer climate and/or the competition with other megaherbivores by the end of the Early Pleistocene (Wang et al., 2014b; Zhang et al., 2016). Recent evidence

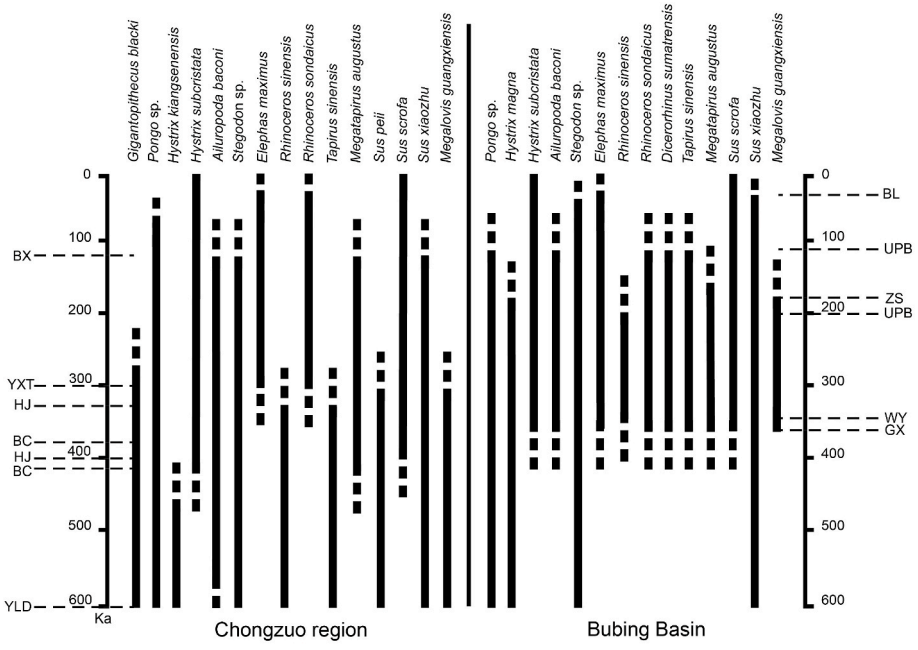

Fig. 10. Comparative records of some typical taxa in the Chongzuo region and in the Bubing basin at the Middle to Late Pleistocene transitional period. Data from the Chongzuo are from Yanlidong Cave (YLD) (~600 ka), Hejiang Cave (HJ) (400–320 ka), Black Cave (BC) (404–382 ka), Yixiantian Cave (YXT) (~300 ka) and Baxian Cave (BX) (~128 ka). Data from the Bubing Basin are from Ganxian Cave (GX) (362–168.9 ka), Upper Pubu Cave (UPB) (200–120 ka), Zhongshan Cave (ZS) (~184 ka), and Baolai Cave (BL) (54–24 ka).

indicates that the latest Neogene Chalicotheridae taxon, *Hesperotherium*, went extinct in mid-Early Pleistocene (1.24 Ma) (Chen et al., 2017). In the Bubing Basin, it is present only in Mohui Cave ~1.7 Ma (Wang et al., 2014a). The Early Pleistocene cave deposits in the Bubing Basin also contain three Neogene Artiodactyla relict species: *Dorcabune liuchengense* (Dong and Bai, 2021), *Cervus* (*Cervavitus*) *fenqii* (Dong, 2011), and *Hippopotamodon ultimus* (Dong and Zhang, 2014), which are typical elements associated with *Gigantopithecus*. While the timing of disappearance of the three ungulate taxa in the Middle Pleistocene remains uncertain, we know that *Gigantopithecus* persisted in China until the late Middle Pleistocene, based on an estimated extinction window of 295–215 ka (Zhang et al., 2024). Current fossil evidence indicates that this ancient Asian Ponginae vanished from the Bubing Basin earlier than from the Chongzuo area, possibly before the advent of the Middle Pleistocene. Indeed, we note its absence in the Ganxian and Zhongshan caves, although it still appeared in the Chongzuo region up to around 255 ka (Zhang et al., 2024).

Based on current knowledge, two archaic taxa of the *Ailuropoda-Stegodon* faunal unit, the small-sized felid, *Felis teilhardi,* and the large-sized cervid, *Cervus* (*Rusa*) *yunnanensis*, may have inhabited only Early Pleistocene ecosystems. As a native species of southern China, *Megalovis guangxiensis* went extinct by the end of the Middle Pleistocene. Initially considered as a key-species of Early Pleistocene faunas, the large-sized porcupine *Hystrix magna* is recorded in the late Middle Pleistocene at Zhongshan and in southeast Guangxi until the Late Pleistocene (Fan et al., 2022b). Similarly, *Sus xiaozhu* which occurred in the Early Pleistocene has been recently identified in the Late Pleistocene Baolai cave (Fan et al., 2022a).

In some lineages, evidence suggests evolutionary changes from Early Pleistocene archaic taxa in the Bubing Basin. As one of the typical members of the "*Ailuropoda-Stegodon*" fauna, the Pleistocene distribution range of the giant panda *Ailuropoda* extended over southern China. The fossil remains indicate that the body size of *Ailuropoda* increased from the Early Pleistocene to the Middle Pleistocene and decreased afterwards (Pei, 1965). In the Bubing Basin, this trend is evident in the replacement of *A. microta* by *A. baconi* which survived into the Late Pleistocene, whereas there is still no convincing data for this pattern in the Chongzuo region.

The Early Pleistocene canid *Sinocuon dubius* (Liao et al., 2023) is considered as the potential ancestor of *Cuon alpinus* of larger body size (Kretzoi, 1941; Qiu et al., 2004), although evidence for a genetic relationship is lacking. *Cuon alpinus* replaced *S. dubius* in the Bubing Basin during the Middle Pleistocene.

Chen (2011) assigned the Early Pleistocene *Stegodon* species to *S. huananensis*. During the Middle Pleistocene, *S. huananensis* evolved into *S. orientalis* with a smaller body mass (Wang et al., 2017a). *S. orientalis* shows an increased number of lophes on the M3/m3, abundant cement covering the crown, and mesostria only present on the first loph of the molars (Chen, 2011).

The most widely distributed rhinoceros in southern China is *Rhinoceros sinensis* (Colbert and Hooijer, 1953; Tong, 2001; Zheng, 2004), which has a close affinity to *R. unicornis* (Antoine, 2012). However, because of a great degree of intraspecific variation, the validity of *R. sinensis* has been questioned (Chen et al., 2012). Based on fossils from Yanliang Cave, Yan et al. (2014) defined a new species, *R. fusuiensis*, which is also considered as a potential ancestor of the living *R. sondaicus*. The rhinoceros from the Bubing Basin assigned to *R. fusuiensis*, which occurred during the early part of the Pleistocene (Wang et al., 2014b; Liao et al., 2023), might have evolved into *R. sondaicus* during the Middle Pleistocene.

Two archaic *Tapirus* species*, T. sanyuanensis and T. peii,* are recorded in southern China during the early stage of the Pleistocene. However, whether the Middle Pleistocene *T. sinensis* derived from the first or the second taxon is still under debate (Tong et al., 2002; 2005b). It was proposed that *T. sinensis* and *Megatapirus augustus* of younger age might be closely related, with the latter species resulting from the former (Tong and Xu, 2001). In the Bubing Basin fossil record, the sequence *T. sanyuanensis–T. sinensis–M. augustus* is present. In relation to wild pigs, *S. scrofa* succeeded from *S. peii* after the Early Pleistocene.

For some taxa, our understanding of their evolutionary history is still limited. For instance, *Pongo* is so far only recorded in the Bubing Basin until the late Middle Pleistocene, while it survived into the Late Pleistocene in Chongzuo (Liao et al., 2022). The extinct *Pongo* species in southern China, only known from isolated teeth which are significantly larger than those of modern taxa *(P. pygmaeus, P. abelii, P. tapanuliensis*) (Xu and Arnason, 1996; Nater et al., 2017), is generally identified as *P. weidenreichi* (Hooijer, 1948; Harrison et al., 2014, 2021). Based mainly on the smaller size of the teeth, the Zhongshan cave specimens were assigned to *P. devosi* (Liang et al., 2024) which is thus far, the only known occurrence of this species in southern China.

Two medium-sized porcupines belonging to the genus *Hystrix*, *H. kiangsenensis* and *H. subcristata*, overlap largely in dental size, making species identification difficult based on isolated teeth. Occurring in the Early to Middle Pleistocene (Zheng, 2004), *H. kiangsenensis* has a larger skull and larger teeth (Van Weers and Zheng, 1998). The fossil record indicates that in the Middle Pleistocene, *H. kiangsenensis* has been replaced by the extant *H. subcristata* in the Bubing Basin.

The large-sized badger, *Meles magnus,* is only found in Early Pleistocene assemblages, whereas *Meles leucurus* is recorded in the late Middle Pleistocene Zhongshan Cave.

In southern China, fossil hyaenids were mostly attributed to the giant *Pachycrocuta* (Huang, 1989). The evolutionary pattern is from *P. brevirostris licenti* to *P. b. sinensis* (Liu et al., 2021). The oldest taxon *P. licenti* (as identified at Chuifeng) lived in the Bubing Basin during the Early Pleistocene without replacement locally by *P. sinensis,* though the record is a bit fragmented. It was later replaced by *Crocuta ultima*.

Seven modern taxa are recorded in the Bubing Basin over the entire Pleistocene. At the genus level, one can cite *Macaca, Hylobates, Muntiacus* and *Capricornis* that *are* likely represented by multiple species (SI-Table 2). At the species level, *Ursus thibetanus, Panthera pardus, Arctonyx collaris* and *Rusa unicolor* are common over the same period, some tentatively identified at a subspecies (infraspecific) level.

Macaques are the most common primates in Southeast Asia. The six extant *Macaca* species are almost similar in dental pattern and size, which makes it difficult for researchers to identify the different species (Corbet and Hill, 1992; Fooden, 1980). The fossil specimens are therefore usually assigned to the genus (e.g. Liang et al., 2020; 2022; Liao et al., 2023; Fan et al., 2022a) with no possibilities to discuss the evolutionary events which occurred in the lineage, and likewise for *Hylobates*.

The fossil badgers are generally larger than the modern forms and the taxon from Yenchingkuo has been assigned to the subspecies *Arctonyx collaris rostratus* (Matthew and Granger, 1923; Colbert and Hooijer, 1953). However, due to the overlapping size ranges with remains from other sites in Southeast Asia, researchers prefer to attribute them to *A. collaris* (e.g. Bacon et al., 2008; Suraprasit et al., 2020).

R. unicolor is considered to originate from *R. yunnanensis* (Zhang and Tong, 2020) in the Early Pleistocene and survived in the Bubing Basin until the Late Pleistocene. The genus *Muntiacus* includes several species and is abundantly represented, yet the evolutionary history of the lineage is unclear due to the difficulty in identifying taxa at the species level.

Although the subfamily Bovinae is very diverse and has a long history in the Bubing Basin itsevolutionary history remains unknown because of very scarce findings.

Some taxa seem to have inhabited the Bubing Basin for a shorter period. For instance, the occurrence of the small bear species, *Helarctos malayanus*, and that of the canid, *Canis* sp., are rare, and the Zhongshan Cave record is the only one in the Bubing Basin to include both taxa. *Panthera tigris* and *Neofelis nebulosa* occurred in the Middle to Late Pleistocene. *Elephas maximus* occurred for the first time in the Middle Pleistocene Ganxian cave deposits of the Bubing Basin (Liang et al.,

2022), which represents the earliest record in southern China (Fig. 10). However, it is absent in the Late Pleistocene caves of Luna and Baolai, whereas widely spread in other regions as a typical member of Late Pleistocene faunas (Wang et al., 2017a, 2017c). We note also the absence of the more archaic *E. kiangnanensis* (Pei, 1987) in this area. Compared to the mixed feeder and more generalist *Elephas*, the browser *Stegodon –S. huananensis* evolved into *S. orientalis*– probably found more favorable forested conditions in the Bubing Basin (Ma et al., 2019).

The unique occurrence of *Equus* in Chuifeng cave represents the southernmost record of the northern genus (Liao et al., 2023). The other genus of the family Rhinocerotidae, *Dicerorhinus*, is recorded only in the Middle Pleistocene assemblages (Liang et al., 2022).

Figure 10 illustrates comparative records of some taxa for the last 600,000 years in the Bubing Basin and Chongzuo region. Despite the fragmented fossil record, the data presented here contributes to refining the biochronological sequence for the region. Overall, the results indicate that, in the interval ~400–200 ka, southern Chinese megafaunas was highly impacted. This could be the consequence of major changes in both the Asian monsoon and global climate, after the Mid-Brunhes event (Cheng et al., 2016). Another decline in megafauna occurred around 120 ka, likely induced by climate shifts (Wang et al., 2008), but uncertainties remain given the fragmented nature of the record. Indeed, we note notable differences between areas: some taxa, *Pongo devosi*, *Hystrix magna, Stegodon orientalis, Rhinoceros sinensis, Sus xiaozhu*, *Megatapirus augustus*, and *Megalovis guangxiensis* survived apparently longer in the Bubing Basin than in the Chongzuo area (Fig. 10). *Elephas kiangnanensis,* which appeared in the Zhiren cave (Jin et al., 2009), has not been found in the Bubing Basin and no records of *Dicerorhinus sumatrensis* have been reported in the Chongzuo region.

These comparative records provide a basis for further discussion on the evolution of faunas from the Middle to Late Pleistocene in southern China. This raises particular questions about the characteristics of the Bubing Basin locally: due to the geomorphology of the region, the Bubing Basin forms a naturally closed basin and it remains to be demonstrated if the landscape favored the longevity of some taxa due to particular environmental conditions. Alternatively, it could be due to a bias in the paleontological record for this transitional period, Bubing being more intenstively studied than Chongzuo. To this respect, a more complete carbon and oxygen isotopic record will be essential to understand the diversity of past environments of southern China.

6. Conclusion

The Zhongshan fauna represents a typical late Middle Pleistocene "*Ailuropoda-Stegodon*" assemblage, as shown by its species composition, and a coupled ESR/U-series dating of a rhinoceros tooth to 184 ± 16 ka. It consists of 33 large-to medium-sized mammals with 5 extinct and 28 extant genera or species, a composition relatively similar to that of the older Ganxian fauna (362–168.9 ka) in the Bubing Basin. Our study also provides a more detailed overview of the history of some mammalian taxa throughout the Pleistocene in the Bubing Basin.

These new data also contribute to improving our understanding of the mammalian evolutionary history in southern China. The transitional period from the Middle to Late Pleistocene is particularly explored by comparing the paleontological records of the Bubing Basin with those of the Chongzuo region. Overall, results highlight two major phases in the decline of megafauna, which require further accuracy with more comprehensive data. Thus, our results provide an updated biochronological background for further analyses of the region.

CRediT authorship contribution statement

Yaobin Fan: Writing – review & editing, Writing – original draft, Formal analysis, Data curation, Conceptualization. **Yanyan Yao:** Formal analysis, Data curation. **Anne-Marie Bacon:** Writing – review & editing, Formal analysis. **Thijs van Kolfschoten:** Writing – review & editing. **Jinyan Li:** Investigation, Data curation. **Christopher J. Bae:** Writing – review & editing. **Wei Liao:** Supervision, Resources, Investigation, Funding acquisition. **Wei Wang:** Writing – review & editing, Supervision, Resources, Funding acquisition, Conceptualization.

Data availability

Research data are available on request (wangw@sdu.edu.cn).

Declaration of competing interest

The authors declare no competing interests.

Acknowledgments

We thank F. Tian from the Tiandong County Museum, C.L. Huang, S. W. Xie and Y.Q. Liufu from Natural History Museum of Guangxi for their participation in the field investigations and excavations, as well as the assistance with specimen sorting and analysis. This work has been supported by Major Program of National Social Science Foundation of China (20&ZD246), National Natural Science Foundation of China (42002025), and the Taishan Scholars Project Special Funds.

Appendix A. Supplementary data

Supplementary data to this article can be found online at https://doi.org/10.1016/j.quaint.2024.11.005.

References

Ansorge, H., Stubbe, M., 1995. Nonmetric skull divergence in the otter-assessing genetic insulation of populations. IUCN Otter Spec. Group Bull. 11, 17–28.
Antoine, P.-O., 2012. Pleistocene and Holocene rhinocerotids (mammalia, Perissodactyla) from the indochinese Peninsula. C. R. Palevol 11, 159–168.
Bacon, A.-M., Demeter, F., Duringer, P., Helm, C., Bano, M., Long, V.T., Thuy, N.K., Antoine, P.-O., Mai, Bui Thi, Huong, Nguyen Thi Mai, Dodo, Y., Chabaux, F., Rihs, S., 2008. The late Pleistocene Duoi U'Oi cave in northern Vietnam: palaeontology, sedimentology, taphonomy and palaeoenvironments. Quat. Sci. Rev. 2, 1627–1654.
Bacon, A.-M., Duringer, P., Antoine, P.-O., Demeter, F., Shackelford, L., Sayavongkhamdy, T., Sichanthongtip, P., Khamdalavong, P., Nokhamaomphu, S., Sysuphanh, V., PatoleEdoumba, E., Chabaux, F., Pelt, E., 2011. The Middle Pleistocene mammalian fauna from Tam Hang karstic deposit, northern Laos: new data and evolutionary hypothesis. Quat. Int. 245, 315–332.
Bacon, A.-M., Westaway, K., Antoine, P.-O., Duringer, P., Blin, A., Demeter, F., Ponche, J.-L., Zhao, J.-X., Barnes, L.M., Sayavonkhamdy, T., Thuy, N.T.K., Long, V. T., Patole-Edouma, E., Shackelford, L., 2015. Late Pleistocene mammalian assemblages of Southeast Asia: new dating, mortality profiles and evolution of the predator-prey relationships in an environmental context. Palaeogeogr. Palaeoclimatol. Palaeoecol. 422, 101–127.
Bacon, A.-M., Antoine, P.-O., Huong, N.T.M., Westaway, K., Tuan, N.A., Duringer, P., Zhao, J., Ponche, J.-L., Dung, S.C., Nghia, T.H., Minh, T.T., Son, P.T., Boyon, M., Thuy, N.T.K., Blin, A., Demeter, F., 2018. A rhinocerotid-dominated megafauna at the MIS6-5 transition: the late middle Pleistocene Coc Muoi assemblage, lang son province, Vietnam. Quat. Sci. Rev. 186, 123–141.
Bae, C.J., Wang, W., Zhao, J., Huang, S., Tian, F., Shen, G., 2014. Modern human teeth from late Pleistocene Luna cave (Guangxi, China). Quat. Int. 354, 169–183.
Bärmann, E.V., Rössner, G.E., 2011. Dental nomenclature in Ruminantia: towards a standard terminological framework. Mamm. Biol. 76, 762–768.
Bien, M.N., Chia, L.P., 1938. Cave and rock-shelter deposits in Yunnan. Bull. Geo. Soc. China. 18, 325–348.
Bocherens, H., Schrenk, F., Chaimanee, Y., Kullmer, O., Mörike, D., Pushkina, D., Jaeger, J.J., 2017. Flexibility of diet and habitat in Pleistocene South Asian mammals: implications for the fate of the giant fossil ape *Gigantopithecus*. Quat. Int. 434, 148–155.
Chen, G., Mo, J., Huang, Z., Tian, F., Huang, W., 2002. Pleistocene vertebrate fauna from Wuyun cave of Tiandong county. Guangxi. Vertebr. Palasiat. 40, 42–51 (in Chinese with English abstract).
Chen, G.F., 2004. Artiodactyla. In: Zheng, S.H. (Ed.), Jianshi Hominid Site. Science Press, Beijing, pp. 1–412.
Chen, G.F., 2011. Remarks on the *Stegodon* from the late Cenozoic of China. Vertebr. Palasiat. 49, 377–392 (in Chinese with English abstract).
Chen, S.K., Huang, W.P., Pei, J., He, C.D., Qin, L., Wei, G.B., Leng, J., 2012. The latest Pleistocene *Stephanorhinus kirchbergensis* from the three gorges area and re-evaluation of Pleistocene rhinos in southern China. Acta Anthropol. Sin. 31, 381–394.

Chen, S., Pang, L., Hu, X., Wei, G., Chen, Y., Ge, R., 2017. New remains of *Hesperotherium* (chalicotheriidae, Perissodactyla) from yanjinggou, wanzhou district, chongqing. Quat. Sci. 37, 166–173.
Chen, S., Wang, J., 2017. Progress in research on tectonic uplift in Yunnan-Guizhou Plateau. Yunnan Geograph. Env. Res. 29, 23–29.
Chen, X., Wu, S., Wang, X., Xu, Q., Shi, H., Li, Q., Jiangzuo, Q., 2023. Discovery of Tang Dynasty smooth-coated otter (*Lutrogale perspicillata*) in Shuyang, Jiangsu, with discussion on its shifting historical distribution. Quat. Sci. 43, 868–877.
Cheng, H., Edwards, R.L., Sinha, A., Spötl, C., Yi, L., Chen, S., Kelly, M., Kathayat, G., Wang, X., Li, X., Kong, X., Wang, Y., Ning, Y., Zhang, H., 2016. The Asian monsoon over the past 640,000 years and ice age terminations. Nature 534, 640–646.
Colbert, E.H., 1943. Pleistocene vertebrates collected in Burma by the American Southeast Asiatic expedition. Trans. Am. Phil. Soc. 32, 395–429.
Colbert, E.H., Hooijer, D.A., 1953. Pleistocene mammals from the limestone fissures of Szechwan, China. Bull. Am. Mus. Nat. Hist. 102, 1–134.
Corbet, G.B., Hill, J.E., 1992. The Mammals of the Indomalayan Region. Natural History Museum Publications. Oxford University Press, Oxford.
de Terra, H., 1938. Preliminary report on recent geological and archaeological discoveries relating to early man in Southeast Asia. Proc. Natl. Acad. Sci. USA 24, 407–413.
Dong, W., 2011. Reconsideration of the systematics of the early Pleistocene *cervavitus* (Cervidae, Artiodactyla, Mammalia). Estud. Geol. 67, 603–611.
Dong, W., Zhang, L., 2014. New materials of *Hippopotamodon* (Artiodactyla, mammalia) from southern China. Vertebr. Palasiat. 52, 201–216.
Dong, W., Bai, W., 2021. Artiodactyla assemblages associated with *Gigantopithecus blacki* in China. Acta Anthropol. Sin. 40, 490–502.
Duringer, P., Bacon, A.-M., Sayavongkhamdy, T., Thuy, N.T.K., 2012. Karst development, breccias history, and mammalian assemblages in Southeast Asia: a brief review. C.R. Palevol 11, 133–157.
Fan, Y., Li, J., Gong, R., Shen, G., Liao, W., Wang, W., 2022a. Taphonomy and biochronology of the late Pleistocene mammalian fauna at Baolai cave, in Bubing Basin, southern China. Hist. Biol. https://doi.org/10.1080/08912963.2022.2145561.
Fan, Y., Shao, Q., Bacon, A.-M., Liao, W., Wang, W., 2022b. Late Pleistocene large-bodied mammalian fauna from Mocun cave in south China: palaeontological, chronological and biogeographical implications. Quat. Sci. Rev. 294, 107741.
Fooden, J., 1980. Classification and distribution of living macaques (*Macaca* Lacépède 1799). In: Lindberg, D.G. (Ed.), The Macaques: Studies in Ecology, Behavior and Evolution. Van Nostrand, New York, pp. 1–9.
Fujita, M., Kawamura, Y., Murase, N., 2000. Middle Pleistocene wild boar remains from NT cave, Niimi, Okayama prefecture, west Japan. J. Geosci. Osaka City Univ. 43, 57–95.
Ge, J.Y., Deng, C., Wang, Y., Shao, Q., Zhou, X., Xing, S., Pang, H., Jin, C., 2020. Climate-influenced cave deposition and human occupation during the Pleistocene in Zhiren Cave, southwest China. Quat. Int. 559, 14–23.
Harrison, T., Jin, C., Zhang, Y., Wang, Y., Zhu, M., 2014. Fossil *Pongo* from the Early Pleistocene *Gigantopithecus* fauna of Chongzuo, Guangxi, southern China. Quat. Int. 354, 59–67.
Harrison, T., Zhang, Y., Yang, L., Yuan, Z., 2021. Evolutionary trend in dental size in fossil orangutans from the Pleistocene of Chongzuo, Guangxi, Southern China. J. Hum. Evol. 161, 103090.
Helgen, K.M., Lim, N.T.L., Helgen, L.E., 2008. The hog-badger is not an edentate: systematics and evolution of the genus *Arctonyx* (Mammalia: Mustelidae). Zool. J. Linn. Soc. 154, 353–385.
Hooijer, D.A., 1948. Prehistoric teeth of man and of the orangutan from central Sumatra, with notes on the fossil orangutan from Java and Southern China. Zool. Meded. 29, 175–301.
Hu, H., Tong, H., Shao, Q., Wei, G., Yu, H., Shi, J., Wang, X., Xiong, C., Lin, Y., Li, N., Wei, Z., Wang, P., Jiangzuo, Q., 2023. New remains of *Ailuropoda melanoleuca baconi* from Yanjinggou, China: throwing light on the evolution of giant pandas during the Pleistocene. J. Mamm. Evol. 30, 137–154.
Huang, W.P., 1989. Taxonomy of the hyaenidae (*Hyaena* and *Crocuta*) of the Pleistocene in China. Vertebr. Palasiat. 27 (3), 197–204 (in Chinese with English summary).
Huang, G., Li, C., Zhao, J., 2018. Development process of layered karst caves and its implication of engineering geology, Wanshouyan, Fujian Province. Quat. Sci. 38, 521–528.
Hwang, Y.T., Larivière, S., 2005. *Lutrogale perspicillata*. Mamm. Species 786, 1–4.
Ji, H., 1977. Division of quaternary mammalian fauna in south China. Vertebr. Palasiat. 4, 271–277.
Jiangzuo, Q., Zhang, B., Deng, L., Chen, X., Wen, J., Tong, H., 2018a. Fossil carnivora (mammalia) from Yangjiawan cave 2, Pingxiang, Jiangxi, with remarks about the tooth identification of quaternary carnivores. In: Dong, Wei (Ed.), Proceedings of the Sixteenth Annual Meeting of the Chinese Society of Vertebrate Paleontology. China Ocean Press, Bejjing, pp. 119–146 (in Chinese).
Jiangzuo, Q., Liu, J., Wagner, J., Chen, J., 2018b. Taxonomical revision of "*Arctonyx*" fossil remains from the liucheng *Gigantopithecus* cave (south China) by means of morphotype and morphometrics, and a review of late Pliocene and early Pleistocene *Meles* fossil records in China. Palaeoworld 27, 282–300.
Jiangzuo, Q., Liu, J., Wagner, J., Dong, W., Chen, J., 2018c. Taxonomical revision of fossil *Canis* in Middle Pleistocene sites of Zhoukoudian, Beijing, China and a review of fossil records of *Canis mosbachensis variabilis* in China. Quat. Int. 482, 93–108.
Jiangzuo, Q., Liu, J., Chen, J., 2019. Morphological homology, evolution, and proposed nomenclature for bear dentition. Acta Palaeontol. Pol. 64, 693–710.
Jiangzuo, Q., 2021. Geographical and chronological distribution of Chinese Pleistocene large canids: current status and prospects. Chin. Sci. Bull. 66, 1426–1440.
Jin, C., Pan, W., Zhang, Y., Cai, Y., Xu, Q., Tang, Z., Wang, W., Wang, Y., Liu, J., Qin, D., Edwards, R.L., Cheng, H., 2009. The *Homo sapiens* cave hominin site of Mulan mountain, Jiangzhou district, Chongzuo, Guangxi with emphasis on its age. Chin. Sci. Bull. 54, 3848–3856.
Jin, C.Z., Wang, Y., Deng, C.L., Harrison, T., Qin, D.G., Pan, W.S., Zhang, Y.Q., Zhu, M., Yan, Y.L., 2014. Chronological sequence of the early Pleistocene *Gigantopithecus* faunas from cave sites in the Chongzuo, zuojiang river area, south China. Quat. Int. 354, 4–14.
Kretzoi, M., 1941. Weitere Beitrage zur Kenntnis der Fauna von Gombaszag. Ann. Hist.-Nat. Mus. Natl. Hung. 34, 105–139.
Li, Y., Wu, M., Peng, S., Zhou, S., 1985. Preliminary report on the investigation of Dingmo cave in Tiandong county, Guangxi. Acta Anthropol. Sin. 4, 127–131 (in Chinese with English abstract).
Liang, H., Liao, W., Shao, Q., Chen, Q., Tian, C., Yao, Y., Wang, W., 2022. New discovery of a late middle Pleistocene mammalian fauna in ganxian cave, southern China. Hist. Biol. https://doi.org/10.1080/08912963.2022.2139180.
Liang, H., Harrison, T., Shao, Q., Bahain, J.-J., Mo, J., Feng, Y., Liao, W., Wang, W., 2024. Evidence for the smallest fossil *Pongo* in southern China. J. Hum. Evol. 189, 103507.
Liang, H., Liao, W., Yao, Y., Bae, C.J., Wang, W., 2020. A late Middle Pleistocene mammalian fauna recovered in northeast Guangxi, southern China: implications for regional biogeography. Quat. Int. 563, 29–37.
Liao, W., Harrison, T., Yao, Y., Liang, H., Tian, C., Feng, Y., Li, S., Bae, C.-J., Wang, W., 2022. Evidence for the latest fossil *Pongo* in southern China. J. Hum. Evol. 107, 103233.
Liao, W., Liang, H., Li, J., Wang, W., 2023. Early Pleistocene large-mammal assemblage associated with *Gigantopithecus* at Chuifeng cave, Bubing Basin, south China. Hist. Biol. https://doi.org/10.1080/08912963.2022.2161381.
Liu, J., Liu, J., Zhang, H., Wagner, J., Jiangzuo, Q., Song, Y., Liu, S., Wang, Y., Jin, C., 2021. The giant short-faced hyena *Pachycrocuta brevirostris* (Mammalia, Carnivora, Hyaenidae) from Northeast Asia: a reinterpretation of subspecies differentiation and intercontinental dispersal. Quat. Int. 577, 29–51.
Ma, J., Wang, Y., Jin, C., Yan, Y., Qu, Y., Hu, Y., 2017. Isotopic evidence of foraging ecology of Asian elephant (*Elephas maximus*) in South China during the late Pleistocene. Quat. Int. 443, 160–167.
Louys, J., Roberts, P., 2020. Environmental drivers of megafauna and hominin extinction in Southeast Asia. Nature 586, 1–5.
Ma, J., Wang, Y., Jin, C., Hu, Y., Bocherens, H., 2019. Ecological flexibility and differential survival of Pleistocene *Stegodon orientalis* and *Elephas maximus* in mainland southeast Asia revealed by stable isotope (C, O) analysis. Quat. Sci. Rev. 212, 33–44.
Maglio, V.J., 1973. Origin and evolution of the elephantidae. Trans. Am. Phil. Soc. 63 (3), 1–149.
Matthew, W., Granger, W., 1923. New fossil mammals from the Pliocene of Szechuan, China. Bull. Am. Mus. Nat. Hist. 48, 563–598.
Nater, A., Mattle-Greminger, M.P., Nurcahyo, A., Nowak, M.G., de Manuel, M., Desai, T., Groves, C., Pybus, M., Sonay, T.B., Roos, C., Lameira, A.R., Wich, S.A., Askew, J., Davila-Ross, M., Fredriksson, G., de Valles, G., Casals, F., PradoMartinez, J., Goossens, B., Verschoor, E.J., Warren, K.S., Singleton, I., Marques, D.A., Pamungkas, J., Perwitasari-Farajallah, D., Rianti, P., Tuuga, A., Gut, I.G., Gut, M., Orozco-terWengel, P., van Schaik, C.P., Bertranpetit, J., Anisimova, M., Scally, A., Marques-Bonet, T., Meijaard, E., Krützen, M., 2017. Morphometric, behavioral, and genomic evidence for a new orangutan species. Curr. Biol. 27, 3487–3498.
Nelson, S.V., 2014. The paleoecology of early Pleistocene *Gigantopithecus blacki* inferred from isotopic analyses. Am. J. Phys. Anthropol. 155, 571–578.
Norton, C.J., Jin, C.Z., Wang, Y., Zhang, Y.Q., 2010. Rethinking the palearctic-oriental biogeographic boundary in quaternary China. In: Norton, C.J., Braun, D. (Eds.), Asian Paleoanthropology: from Africa to China and beyond. Vertebrate Paleobiology and Paleoanthropology Series. Springer Press, Dordrecht, The Netherlands, pp. 81–100.
Pan, Y., 2021. An α-taxonomy Study of the Late Middle Pleistocene Mammalian Fauna from the Yixiantian Cave, Chongzuo, Guangxi Zhuang Autonomous Region. Thesis of University of Chinese Academy of Sciences.
Pan, Y., Zhang, Y., Yang, L., Takai, M., Harrison, T., Westaway, K., Jin, C., 2023. Preliminary description of a late Middle Pleistocene mammalian fauna prior to the extinction of *Gigantopithecus blacki* from the Yixiantian cave, Guangxi ZAR, south China. Anat. Rec. 2023, 1–26.
Patte, E., 1928. Comparaison des faunes de mammifères de Langson (Tonkin) et du SE Tchouen. Bull. Soc. Geol. Fr. 28, 55–63.
Pei, W., 1965. More on the problem of augmentation and diminution in size of Quaternary mammals. Vertebr. Palasiat. 9, 37–46 (in Chinese with English abstract).
Pei, W., 1987. Carnivora, Proboscidea and Rodentia from Liucheng *Gigantopithecus* cave and other caves in Guangxi (in Chinese with English abstract). Mem. Inst. Vertebr. Paleontol. Paleoanthropol. Acad. Sinica 18, 1–134.
Pope, G.G., Frayer, D.W., Liangchareon, M., Kulasing, P., Nakabanlang, S., 1981. Palaeoanthropological Investigations of the Thai-American Expeditions in Northern Thailand (1978-1980): an Interim Report, vol. 21. Asian Perspect, pp. 147–163.
Qiu, Z., Deng, T., Wang, B., 2004. Early Pleistocene Mammalian Fauna from Longdan, Dongxiang, Gansu, China. Science Press, Beijing, pp. 1–193 (in Chinese).
Rink, W.J., Wei, W., Bekken, D., Jones, H.L., 2008. Geochronology of *Ailuropoda-Stegodon* fauna and *Gigantopithecus* in Guangxi province, southern China. Quat. Res. 69, 377–387.
Roth, V.L., Shoshani, J., 1988. Dental identification and age determination in *Elephas maximus*. J. Zool. (Oxf.) 214 (4), 567–588.
Schwartz, J.H., Long, V.T., Cuong, N.L., Kha, L.T., Tattersall, I., 1995. A review of the Pleistocene hominoid fauna of the Socialist Republic of Vietnam (excluding Hylobatidae). Anthropol. Pap. Am. Mus. Nat. Hist. 76, 1–24.

Shao, Q., Wang, W., Deng, C., Voinchet, P., Lin, M., Zazzo, A., Douville, E., Dolo, J., Falguères, C., Bahain, J.J., 2014. ESR, U-series and paleomagnetic dating of *Gigantopithecus* fauna from Chuifeng Cave, Guangxi, southern China. Quat. Res. 82, 270–280.

Stacklyn, S., Wang, Y., Jin, C., Wang, Y., Sun, F., Zhang, C., Jiang, S., Deng, T., 2017. Carbon and oxygen isotopic evidence for diets, environments and niche differentiation of Early Pleistocene pandas and associated mammals in South China. Palaeogeogr. Palaeoclimatol. Palaeoecol. 468, 351–361.

Sun, L., Deng, C., Wang, W., Liu, C., Kong, Y., Wu, B., Liu, S., Ge, J., Qin, H., Zhu, R., 2017. Magnetostratigraphy of Plio-Pleistocene fossiliferous cave sediments in the Bubing Basin, southern China. Quat. Geochronol. 37, 68–81.

Sun, J.-J., Zhang, B., Chen, X., Deng, L., Wen, J., Tong, H.-w., 2021. New fossils of Late Pleistocene *Sus scrofa* from Yangjiawan cave 2, Jiangxi, China. Vertebr. Palasiat. 59 (1), 64–80.

Suraprasit, K., Jaeger, J.-J., Chaimanee, Y., Chavasseau, O., Yamee, C., Tian, P., Panha, S., 2016. The Middle Pleistocene vertebrate fauna from Khok Sung (Nakhon Ratchasima, Thailand): biochronological and paleobiogeographical implications. ZooKeys 613, 1–157.

Suraprasit, K., Jaeger, J.-J., Chaimanee, Y., Sutcharit, C., 2020. Taxonomic reassessment of large mammals from the Pleistocene *Homo*-bearing site of Tham Wiman Nakin (northeast Thailand): relevance for faunal patterns in mainland southeast Asia. Quat. Int. 603, 90–112.

Swindler, D.R., 2002. Primate Dentition. Cambridge University Press, Cambridge.

Takai, M., Zhang, Y., Kono, R.T., Jin, C., 2014. Changes in the composition of the Pleistocene primate fauna in southern China. Quat. Int. 354, 75–85.

Tian, C., Liao, W., Yao, Y., Seong, C., Bae, C.-J., Wang, W., 2020. Human behavioral responses to the 8.2 ka BP climatic event: archaeological evidence from the Zhongshandong cave site in Bubing Basin, Guangxi, southern China. Quat. Int. 563, 96–104.

Tong, H., 2001. Rhinocerotids in China - systematics and material analysis. Geobios 34, 585–591.

Tong, H., 2005a. *Hystrix subcristata* (Mammalia, Rodentia) from Tianyuan Cave, a human fossil site newly discovered near Zhoukoudian (Choukoutien). Vertebr. Palasiat. 43 (2), 135–150.

Tong, H., 2005b. Dental characters of the Quaternary tapirs in China, their significance in classification and phylogenetic assessment. Geobios 38, 139–150.

Tong, H., 2008. Quaternary *Hystrix* (Rodentia, Mammalia) from north China: taxonomy, stratigraphy and zoogeography, with discussions on the distribution of *Hystrix* in palearctic eurasia. Quat. Int. 179 (1), 126–134.

Tong, H., Xu, F., 2001. On the origin and evolution of Quaternary tapirs in China. In: Wang, Y., Deng, T. (Eds.), Proceedings of the Eighth Annual Meeting of the Chinese Society of Vertebrate Paleontology. China Ocean Press, Beijing, pp. 133–141 (in Chinese with English abstract).

Tong, H., Liu, J., Han, L., 2002. On fossil remains of early Pleistocene tapir (Perissodactyla, Mammalia) from Fanchang, Anhui. Chin. Sci. Bull. 47, 586–590.

van der Made, J., 1996. Listriodontinae (Suidae, Mammalia), their evolution, systematics and distribution in time and space. Contrib. Tert. Quat. Geol. 33 (1–4), 3–254.

van Weers, D.J., 1990. Dimensions and occlusal pattern in molars of *Hystrix brachyura* Linnaeus, 1758 (Mammalia, Rodentia) in a system of wear categories. Bijdr. Dierkd. 60, 121–134.

van Weers, P.J., Zheng, S.H., 1998. Biometric analysis and taxonomic allocation of Pleistocene *Hystrix* specimens (Rodentia, porcupines) from China. Beaufortia 48, 47–69.

Wang, Y., Cheng, H., Edwards, R.L., Kong, X., Shao, X., Chen, S., Wu, J., Jiang, X., Wang, X., An, Z., 2008. Millennial- and orbital-scale changes in the East Asian monsoon over the past 224,000 years. Nature 451, 1090–1093.

Wang, W., Potts, R., Baoyin, Y., Huang, W., Cheng, H., Edwards, R.L., Ditchfield, P., 2007. Sequence of mammalian fossils, including hominoid teeth, from the Bubing Basin caves, South China. J. Hum. Evol. 52, 370–379.

Wang, W., 2009. New discoveries of *Gigantopithecus blacki* teeth from Chuifeng cave in the Bubing Basin, Guangxi, south China. J. Hum. Evol. 57, 229–240.

Wang, W., Liao, W., Li, D., Tian, F., 2014a. Early Pleistocene large-mammal fauna associated with *Gigantopithecus* at Mohui cave, Bubing Basin, south China. Quat. Int. 354, 122–130.

Wang, Y., Wei, G., Mead, J.I., Jin, C., 2014b. First mandible and deciduous dentition of juvenile individuals of *Sinomastodon* (Proboscidea, mammalia) from the early Pleistocene Renzidong cave of eastern China. Quat. Int. 354, 131–138.

Wang, Y., Jin, C., Mead, J., 2014c. New remains of *Sinomastodon yangziensis* (Proboscidea, Gomphotheriidae) from Sanhe karst cave, with discussion on the evolution of Pleistocene Sinomastodon in south China. Quat. Int. 339–340, 90–96.

Wang, W., Zhao, L., Du, B., Zhang, L., Wang, X., Cai, H., 2017a. New proboscidean remains associated with *Homo sapiens* from the mawokou cave in Bijie, Guizhou province of south-western China. Acta Anthropol. Sin. 36, 414–425.

Wang, Y., Jin, C., Pan, W., Qin, D., Yan, Y., Zhang, Y., Liu, J., Dong, W., Deng, C., 2017b. The early Pleistocene *gigantopithecus-sinomastodon* fauna from Juyuan karst cave in Boyue mountain, Guangxi, south China. Quat. Int. 434, 4–16.

Wang, Y., Qin, D., Jin, C., 2017c. New Elephas remains from the Zhiren cave of Mulan mountain, Chongzuo, Guangxi with discussion on quaternary proboscidean evolution in southern China. Quat. Sci. 37, 854–859.

Xu, X., Arnason, U., 1996. The mitochondrial DNA molecule of Sumatran orangutan and a molecular proposal for two (Bornean and Sumatran) species of orangutan. J. Mol. Evol. 43, 431–437.

Yan, Y., Wang, Y., Jin, C., Mead, J.I., 2014. New remains of rhinoceros (rhinocerotidae, Perissodactyla) associated with *Gigantopithecus blacki* from the early Pleistocene Yanliang cave, Fusui, south China. Quat. Int. 354, 111–121.

Yao, Y., Fan, Y., Bae, C.-J., Tian, C., Liang, H., Chen, J., Zhang, B., Wei, S., Shao, Q., Liao, W., Wang, W., 2023. Early mid-pleistocene mammal fauna from Yanlidong cave, south China. Hist. Biol. https://doi.org/10.1080/08912963.2023.2185886.

Zhang, H., Wang, Y., Janis, C.M., Goodall, R.H., 2016. An examination of feeding ecology in Pleistocene proboscideans from southern China (*Sinomastodon, Stegodon, Elephas*), by means of dental microwear texture analysis. Quat. Int. https://doi.org/10.1016/j.quaint.2016.07.011.

Zhang, Y., Harrison, T., 2017. Gigantopithecus blacki: a giant ape from the Pleistocene of Asia revisited. Am. J. Phys. Anthropol. 162, 153–177.

Zhang, B., Chen, X., Tong, H.W., 2018. Tooth remains of Late Pleistocene moschid and cervid (Artiodactyla, mammalia) from Yangjiawan and Fuyan caves of southern China. Quat. Int. 490, 21–32.

Zhang, B., Tong, H., 2020. New fossils of sambar (*Rusa unicolor*) from Bailong cave, a Middle Pleistocene human site in Hubei, China. Quat. Int. 550, 120–129.

Zhang, Y., Westaway, K.E., Haberle, S., Lubeek, J.K., Bailey, M., Ciochon, R., Morley, M. W., Robert, R., Zhao, J., Duval, M., Dosseto, A., Pan, Y., Rule, S., Liao, W., Gully, G. A., Lucas, M., Mo, J., Yang, L., Cai, Y., Wang, W., Joannes-Boyau, R., 2024. The demise of the giant ape *Gigantopithecus blacki*. Nature 625, 535–539.

Zheng, S., 2004. Jianshi Hominid Site. Science Press, Beijing (in Chinese with English summary).

Zhou, M., 1957. The nature and contrast of Tertiary and Early Quaternary mammalian fauna in South China. Chin. Sci. Bull. 13, 394–400.

Zhou, D., Liu, X., Jiang, L., Liu, C., 2005. Step-like landforms and uplift of Guizhou Plateau. Earth Environ. 33, 79–84.